

INVESTIGATION OF THE FORMATION AND BEHAVIOR
OF CLOGGING MATERIAL IN EARTH AND
SPACE STORABLE PROPELLANTS

FINAL REPORT 08113-6025-R000

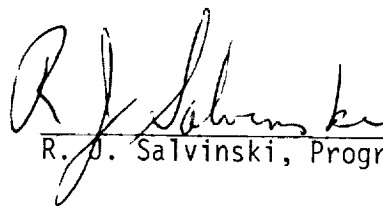
NOVEMBER 1969

Prepared for


THE JET PROPULSION LABORATORY
PASADENA, CALIFORNIA 91103
UNDER NATIONAL AERONAUTICS AND SPACE
ADMINISTRATION CONTRACT NAS 7-549

TRW SYSTEMS GROUP
ONE SPACE PARK
REDONDO BEACH
CALIFORNIA

Prepared for
THE JET PROPULSION LABORATORY
PASADENA, CALIFORNIA 91103
Under NATIONAL AERONAUTICS AND SPACE
ADMINISTRATION CONTRACT NAS 7-549



R. J. Salvinski, Program Manager

Approved 

H. L. Burge, Manager
Applied Technology Department

Approved 

E. A. Burns, Manager
Chemical Research and Services
Department

Approved 

D. H. Lee, Manager
Technology Laboratory

TRW SYSTEMS GROUP

FOREWORD

This report was prepared by TRW Systems Group, Redondo Beach, California, and represents the program efforts between 9 October 1968 and 9 November 1969. The work was performed under NASA Contract NAS 7-549 for the purpose of studying the phenomenon of the formation of clogging material in rocket propellants under flow conditions. The program was originated and managed by the Jet Propulsion Laboratory under the technical direction of Mr. Louis R. Toth. The NASA Program Manager is Mr. Frank E. Compitello, Code RPL, Office of Advanced Research and Technology.

The work performed on the program was accomplished by the Science and Technology Division of TRW Systems Group. Technical direction of the program is provided by the Applied Technology Department of the Technology Laboratory. The program manager is Mr. R. J. Salvinski. Responsible technical personnel are Dr. E. A. Burns, Mr. M. Gardner, Mr. A. Grunt, Mr. J. R. Denson and Dr. J. Neff of the Chemical Research and Services Department, and Mr. J. L. Reger of the Materials Science Department, Physical Research Center. Mr. C. E. Armstrong of the Applied Technology Department was responsible for Instrumentation and Data Reduction.

CONTENTS

	<u>Page</u>
1.0 INTRODUCTION AND SUMMARY	1-1
1.1 Objectives	1-2
1.2 Specific Tasks	1-2
1.3 Summary	1-5
1.3.1 Recommendations	1-5
2.0 CORROSIVITY OF OXYGEN DIFLUORIDE AND DIBORANE (Task 1)	2-1
2.1 Introduction	2-1
2.2 Test Facilities	2-1
2.3 Selected Materials and Propellant Dopants	2-1
2.3.1 OF ₂ Dopants	2-3
2.3.2 B ₂ H ₆ Dopants	2-4
2.3.3 Storage Containers	2-4
2.3.4 Corrosion Specimens	2-6
2.4 Test Procedures	2-6
2.5 Metallurgical Examination of Specimens	2-7
3.0 CHARACTERIZATION OF OXYGEN DIFLUORIDE AND DIBORANE (Task 2)	3-1
3.1 Introduction	3-1
3.2 Analyses of OF ₂ and B ₂ H ₆	3-1
3.2.1 Chemical Analyses of Oxygen Difluoride	3-2
3.2.2 Chemical Analyses of Diborane	3-4
3.3 Laser Examination of OF ₂ and B ₂ H ₆	3-7
3.3.1 Laser Characterization of OF ₂	3-10
3.3.2 Laser Characterization of B ₂ H ₆	3-12
4.0 PROPELLANT FLOW TESTING (Task 3)	4-1
4.1 Introduction	4-1
4.2 Oxygen Difluoride/Diborane Flow Tests	4-1
4.2.1 Flow System	4-1
4.2.2 Instrumentation	4-8
4.2.3 Procedures and Operating Conditions	4-11

Contents (Continued)

	<u>Page</u>
4.2.4 Propellant Sources	4-13
4.2.5 Diborane Test Results	4-14
4.2.6 Oxygen Difluoride Test Results	4-14
4.3 Hydrazine Flow Testing	4-17
4.3.1 Extrusion Rheometer Test Apparatus	4-17
4.3.2 Hydrazine Test Results	4-20
5.0 ANALYSES OF RESULTS	5-1
5.1 Corrosivity of Oxygen Difluoride and Diborane	5-1
5.1.1 Corrosivity of OF_2	5-1
5.1.2 Corrosivity of B_2H_6	5-2
5.2 Characterization of Oxygen Difluoride and Diborane	5-2
5.2.1 Characterization of OF_2	5-2
5.2.2 Characterization of B_2H_6	5-4
5.3 Propellant Flow Testing	5-5
5.3.1 Oxygen Difluoride Flow Tests	5-5
5.3.2 Diborane Flow Tests	5-6
5.3.3 Hydrazine Flow Tests	5-7

ILLUSTRATIONS

	<u>Page</u>
Figure 2-1. Schematic Diagram of Transfer System and Storage Facility for OF_2 Corrosion Study	2-2
Figure 2-2 Configuration of Storage Container	2-4
Figure 2-3. Comparison of the Longitudinal and Transverse Cross-Section of the Control Specimens Used in the Corrosion Tests	2-9
Figure 2-4. Comparison of the Corrosivity of Diborane and Oxygen Difluoride on 6061-T6 Aluminum	2-10
Figure 2-5. Comparison of the Corrosivity of Diborane and Oxygen Difluoride on 347 Stainless Steel	2-11
Figure 2-6. Comparison of the Corrosivity of Diborane and Oxygen Difluoride on Titanium 6Al-4V Alloy	2-12
Figure 2-7. Comparison of Surface of Titanium 6Al-4V Control with Specimen Exposed to Doped Oxygen Difluoride	2-13
Figure 2-8. Scanning Electron Photomicrographs of 304 Stainless Steel Oxide Powder	2-17
Figure 2-9. Photomicrograph of Stainless Steel Oxides (-325 mesh).	2-20
Figure 3-1. Laser Viewing Assembly	3-8
Figure 3-2. Photograph of Laser Viewing Assembly	3-9
Figure 3-3. Apparatus for Detecting Tyndall Effect	3-10
Figure 4-1. Schematic Diagram of Test Facility for $\text{OF}_2/\text{B}_2\text{H}_6$ Flow System	4-2
Figure 4-2. OF_2 Diborane Test Assembly	4-4
Figure 4-3. Flow Measuring Assembly	4-6
Figure 4-4. Photograph of Capillary Test Section and Filters Used in $\text{OF}_2/\text{B}_2\text{H}_6$ Flow System	4-7
Figure 4-5. Transducer Placement on $\text{OF}_2/\text{B}_2\text{H}_6$ Flow System	4-9
Figure 4-6. Extrusion Rheometer Setup	4-18
Figure 4-7. Capillary Test Section	4-19

TABLES

	<u>Page</u>
Table 2-1. Corrosion Test Specimens	2-5
Table 2-2. Results of Corrosivity Tests on Metal Specimens with Oxygen Difluoride and Diborane Stored for 45 Days	2-8
Table 3-1. Mass Spectrometer Analyses of Diborane	3-5
Table 3-2. Mass Spectrometer Analyses of B_2H_6	3-6
Table 4-1. Operation Conditions and Construction Components for Flow Decay Studies	4-3
Table 4-2. System Measurement Accuracy Run to Run	4-10
Table 4-3. System Measurement Accuracy Within a Single Run	4-10
Table 4-4. Diborane Test Results at $-145^\circ C$	4-15
Table 4-5. Oxygen Difluoride Test Results at $-145^\circ C$	4-16
Table 4-6. Experimental Data	4-21
Table 4-7. Theoretical Hydrazine Flow Rate Data	4-22

1.0 INTRODUCTION AND SUMMARY

The propellants studied during the program include hydrazine, oxygen difluoride and diborane. The program effort represents a continuation of work initiated by TRW Systems Group during January 1967⁽¹⁾. The objective of the original program was to investigate the formation and behavior of flow clogging materials formed when flowing nitrogen tetroxide. The clogging material was identified as a gel material which formed a powdery residue upon drying in air.

A continuation of the original effort was performed during October 1967 to October 1968⁽²⁾. Under this program the propellants studied were the earth storable propellants nitrogen tetroxide and hydrazine and the space storable propellants oxygen difluoride and diborane. Nitrogen tetroxide propellant was subjected to environmental conditions designed to artificially produce clogging material in the propellant. Test methods were also developed which included the use of a low cost flow apparatus and the use of a laser to determine colloidal particles in the propellants.

Results of the earlier work flowing nitrogen tetroxide through filters and capillaries with varying flow rates showed flow degradation to occur in the capillary and filter test runs to the extent of complete clogging and flow stoppage. A gel-like material found at the entrance of both the capillary and filters was responsible for the blockage. Tests were also performed with hydrazine flowed through a .010-inch diameter capillary. No flow decay was found in limited tests flowing hydrazine.

An important part of the above programs included corrosivity tests conducted with both nitrogen tetroxide and hydrazine, and the metal specimens - aluminum, stainless steel, and titanium stored in glass compatibility tubes. The nitrogen tetroxide propellant used in the corrosion tests was conditioned by adding the impurities H_2O , $NOCl$, Cl_2 , $NOCl + O_2$ and O_2 . The hydrazine was conditioned by adding NH_3 , CO_2 and H_2O . The purpose of these tests were

to investigate the role of impurities in propellants on the corrosion of materials and the subsequent effect of corrosion products on the formation of clogging materials.

1.1 OBJECTIVES

It was the objective of the current program to perform a continued investigation of clogging behavior of propellants during flow. The major emphasis was on the propellants oxygen difluoride, diborane and hydrazine and their behavior under dynamic flow conditions.

The scope of the effort included (1) the effect of corrosivity on the characteristics of oxygen difluoride and diborane with selected metals; (2) the chemical characterization of oxygen difluoride and diborane; and (3) the behavior of oxygen difluoride and diborane under dynamic flow conditions.

1.2 SPECIFIC TASKS

The specific tasks of this program were to perform an analysis and laboratory tests directed toward determining the formation and behavior of clogging material in oxygen difluoride and diborane propellants. The impurities considered in this work which may affect the flow characteristics of oxygen difluoride and diborane were limited to those generated by engineering materials typically used in propulsion systems and components.

Design parameters considered were typical of or scalable to those in real systems and components. The objectives were met by performing the following tasks:

Task 1 - Corrosivity of Propellants

Under this task, the corrosivity of liquid oxygen difluoride and diborane on selected metal alloys was investigated. Doped oxygen difluoride and neat diborane were stored with aluminum, stainless steel and titanium for a period of at least one month.

Task 2 - Characterization of Propellants

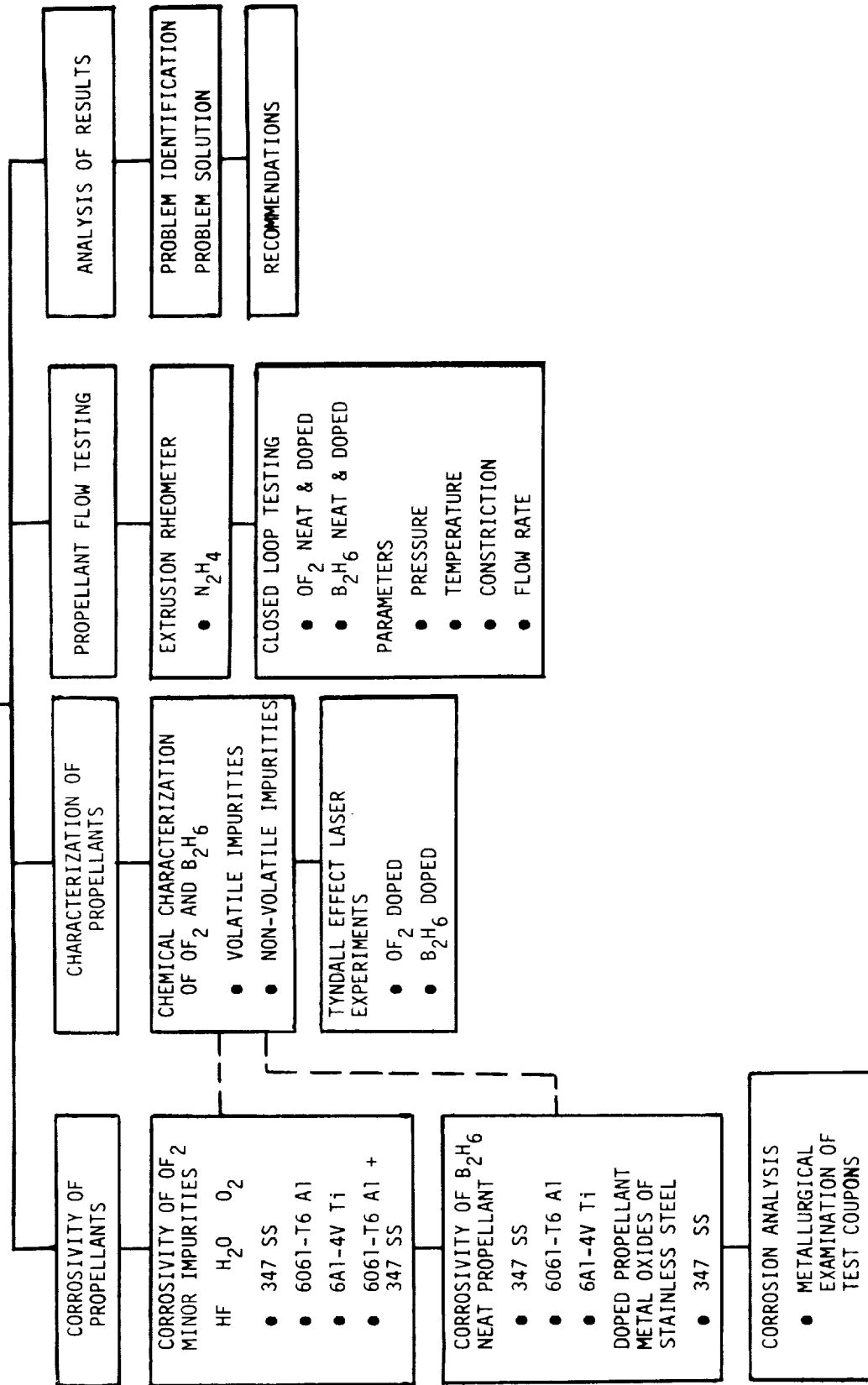
The objective of this task was to investigate the formation and existence of impurities in the form of a suspendable or colloidal material in oxygen difluoride and diborane. The laser technique of determining a Tyndall effect was utilized. The propellants characterized included both neat oxygen difluoride and diborane and oxygen difluoride and diborane contaminated with metal and organic impurities representative of those which might be generated in propulsion systems and components.

Task 3 - Propellant Flow Testing

The objective of this task was to determine the extent of flow degradation and clogging in small clearances under dynamic conditions. Oxygen difluoride and diborane were flowed through a capillary under conditions of varying pressure, temperature and velocity. An additional task was to flow hydrazine through a capillary test section using the extrusion rheometer. The extrusion rheometer used during the previous program was modified to improve heat transfer characteristics.

A detailed work plan of the above tasks is presented in the chart on the following page.

INVESTIGATION OF THE FORMATION AND BEHAVIOR OF CLOGGING MATERIAL IN EARTH AND SPACE STORABLE PROPELLANTS - NAS 7-549



1.3 SUMMARY

No evidence of clogging was found flowing neat OF_2 and neat B_2H_6 through a one-inch long, 0.010-inch diameter capillary. Flow rates through the 0.010-inch capillary varied from 16 ft/sec to 32 ft/sec flowing OF_2 and varied from 22 ft/sec to 44 ft/sec flowing B_2H_6 .

A series of five runs were made flowing specification grade hydrazine through a 0.005-inch diameter capillary, 0.8 inches long. Flow blockage occurred in two runs believed due to particulate contamination. Flow decay was also observed in two other runs, however, at no time was evidence of gel or viscous material found. No apparent cause of the flow decay anomalies was identified, however, partial blockage of the capillary could result from spurious particulate contamination.

Examination of 347 stainless steel, 6Al-4V titanium and 6061 aluminum exposed to liquid OF_2 , doped with HF and O_2 , and stored at -78°C for 45 days, showed the titanium to be the most severely attacked. The stainless steel specimens showed the least attack and aluminum was slightly attacked.

Corrosivity tests with the above metal alloys with neat liquid B_2H_6 at -78°C for 45 days showed aluminum to be most affected, although to a minor degree. Titanium was minimally attacked and stainless steel the least affected. Stainless steel oxides stored with B_2H_6 at -78°C and -20°C for 30 days showed reduction of the oxides to metal. Reduction of the oxides to metal indicates a potential problem area with sliding or dynamic contact of metals such as might be found in bearings and valve poppet seats.

A more detailed discussion of the results and summary is given in Section 5.0.

1.3.1 Recommendations

The study to determine flow behavior of oxygen difluoride and diborane through a 0.010-inch capillary showed no evidence of flow anomalies. A continuation of the effort should include an investigation of the flow

behavior of OF_2 and B_2H_6 through filters and orifices. The filters selected for the study would logically include both the screen type and the disc type filters.

Experiments should be designed to show the effect of suddenly lowering the temperature of propellants prior to entering the flow orifices to determine whether the impurities most likely encountered and not easily removed can cause flow decay. Precipitation, if possible, would occur under these conditions. Ideally, flow experiments should utilize conditioned propellant held for extended periods in the selected storage containers. The impurities used as dopants should include metal corrosion products and polymers likely to be considered in the construction of propulsion systems.

In addition to investigating liquid diborane flow behavior, the formation of yellow solids (pyrolysis) in gaseous diborane should be studied. Heating of the propulsion components due to heat soakback or in circulating cooling systems can result in pyrolysis solids in the propellant which may be deposited at constrictions during flow.

The formation of B_2H_6 "ice" during flow through orifices is another form of clogging phenomenon. Ice formation is possible, however, proper design of the flow system should alleviate this possibility.

Previous studies have demonstrated that changes of fluid viscosity with temperature can be measured utilizing the present extrusion rheometer configuration. Final verification of the applicability of this design to the observation or measurement of flow decay behavior in fluids must consist of construction and testing of an apparatus for N_2O_4 application where flow decay behavior with capillaries has been characterized.

Future hydrazine flow testing should use capillary sections employing a larger diameter capillary (10 mil for example). The larger bore capillary will be less prone to clogging resulting from extraneous rheometer contamination. The hydrazine flow tests should be conducted with dopants, CO_2 ,

H₂O, metals, plasticizers and residues from hydrazine-material compatibility tests. These suggested dopants are materials which may be exposed to hydrazine through propellant storage and handling.

REFERENCES

1. "Investigation of the Formation and Behavior of Clogging Materials in Earth and Space Storable Propellants," Interim Report 08113-6007-R000, October 1967.
2. "Investigation of the Formation and Behavior of Clogging Materials in Earth and Space Storable Propellants," Interim Report 08113-6016-R000, October 1968.

2.0 CORROSIVITY OF OXYGEN DIFLUORIDE AND DIBORANE (TASK 1)

2.1 INTRODUCTION

The purpose of this task was to investigate the corrosivity of liquid oxygen difluoride (OF_2) and liquid diborane (B_2H_6) propellants in contact with selected metals. The metals were stored with doped liquid oxygen difluoride and neat liquid diborane for a period of more than one month at -78°C . The laboratory tests were designed to provide corrosion data on the metal specimens as well as the effects of corrosion of the selected metals on the chemical and physical properties of the propellants. The materials selected were stainless steel, aluminum and titanium which are considered likely candidates for use in propellant tankage. The liquid propellants were characterized after storage under Task 2, Section 3.0.

2.2 TEST FACILITIES

Because of the extreme toxicity of propellants and the capacity of OF_2 to ignite and burn fuels and metals, low pressure and low temperature vacuum transfer methods were used. The test facility for OF_2 , constructed of 300 series stainless steel lines, valves and fittings, is shown schematically in Figure 2-1. A similar all-glass transfer system, not shown, was used for handling B_2H_6 .

2.3 SELECTED MATERIALS AND PROPELLANT DOPANTS

Liquid oxygen difluoride and diborane were stored for 45 days at -78°C in the presence of the selected specimens to determine the extent of corrosion and corrosion products formed. The propellants were characterized and examined for particulate matter under Task 2, Section 3.0.

Materials chosen for this investigation were those believed to be candidate tankage construction materials. The one exception to this was the selection of a sample of oxides of stainless steel stored in liquid diborane. This was stored because diborane is a very strong reducing agent. The storage conditions for three tests were -78°C for 45 and 30 days and -20°C for 30 days. The possibility exists that certain oxides which are present on all materials of construction could be reduced under these storage conditions.

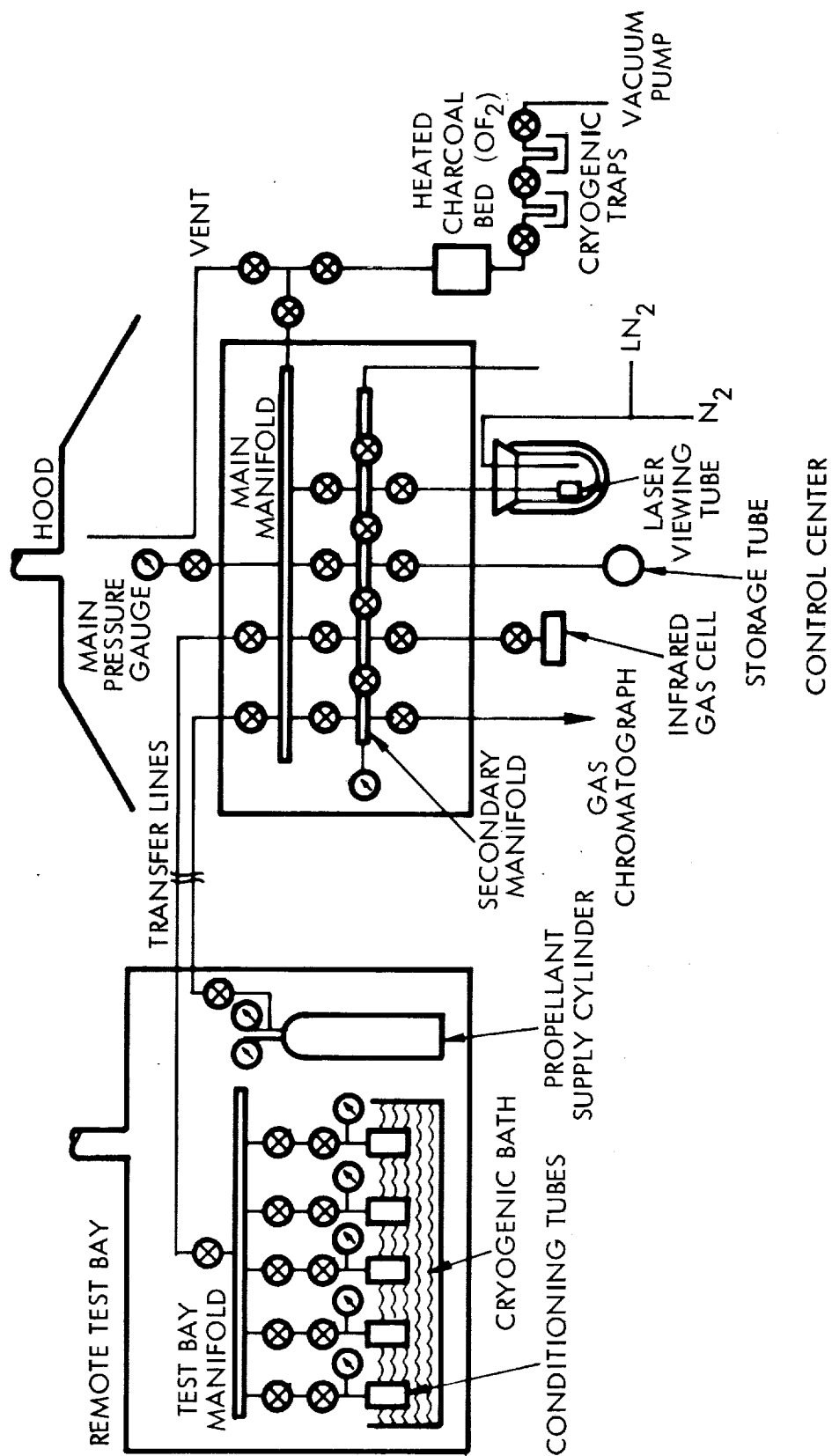


Figure 2-1. Schematic Diagram of Transfer System and Storage Facility for OF_2 Corrosion Study

The choice of selected dopants represented those impurities which were considered to be normal impurities introduced by standard handling procedures and those most likely to be introduced in processing. The metals and propellants used in the corrosion study are shown in the following table:

<u>Oxygen Difluoride</u>		<u>Diborane</u>	
Doped with HF, H ₂ O, O ₂		Neat	
<u>Storage Container</u>	<u>Specimen</u>	<u>Storage Container</u>	<u>Specimen</u>
347 SS	347 SS	347 SS	347 SS
6061-T6 Al	6061-T6 Al	6061-T6 Al	6061-T6 Al
6Al-4V Ti	6Al-4V Ti	6Al-4V Ti	6Al-4V Ti
347 SS	6061-T6 Al	347 SS	Oxides of Stainless Steel*

*Prepared by burning 304 stainless steel shim stock in gaseous oxygen; all oxides used passed a 325 mesh screen.

2.3.1 OF₂ Dopants

The dopants hydrogen fluoride and water were added to oxygen difluoride because they represent the most corrosive additives considered and these are most probable to be encountered. Many reactions can occur and a few of the most probable are listed below:

1. Water would react (the rate, however, is unknown at low temperatures) to produce hydrogen fluoride and oxygen.
2. Hydrogen fluoride could react with metal surfaces to release hydrogen gas. Hydrogen may react further with oxygen difluoride to produce hydrogen fluoride.
3. Hydrogen fluoride readily absorbs on many metal fluoride surfaces.
4. Hydrogen fluoride reacts with some metal fluorides to form complex metal fluorides and may solubilize the protective fluoride coating. These may dislodge and form particulate matter or complex metal fluoride crystals.

2.3.2 B₂H₆ Dopants

In the literature, there is little evidence of massive corrosion of pure metals by liquid diborane, but the effect of these metals on diborane is unknown. For diborane storage, the choice of possible corrosive dopants would thus appear to be limited because diborane is a powerful reducing reagent. Yet diborane has the potential to reduce metal oxides and should not be stored at moderate temperatures in the presence of active metal oxides. Because all metals have a thin coating of oxides, hydroxides or basic metal oxides, the possibility exists that partial reduction of, or hydrolysis of boron hydrides on these surfaces could produce metastable colloidal particles. It is known that water and diborane react to produce boric acid and hydrogen and, therefore, water should be avoided.

For these reasons, metal samples were stored in liquid diborane to determine if any potential clogging agents formed. A sample of oxides of stainless steel was also stored in liquid diborane to determine if surface degradation of the oxide occurs.

2.3.3 Storage Containers

The storage containers were machined from metal stock to approximately the dimensions of a Hoke Inc., Cylinder 2HS10. The capacity of the cylinder was 6ml. The containers were double valved and capped with AN fittings. Dimensions of the storage container are shown in Figure 2-2. The storage containers were prepared and cleaned to the schedule reported in Table 2-1.

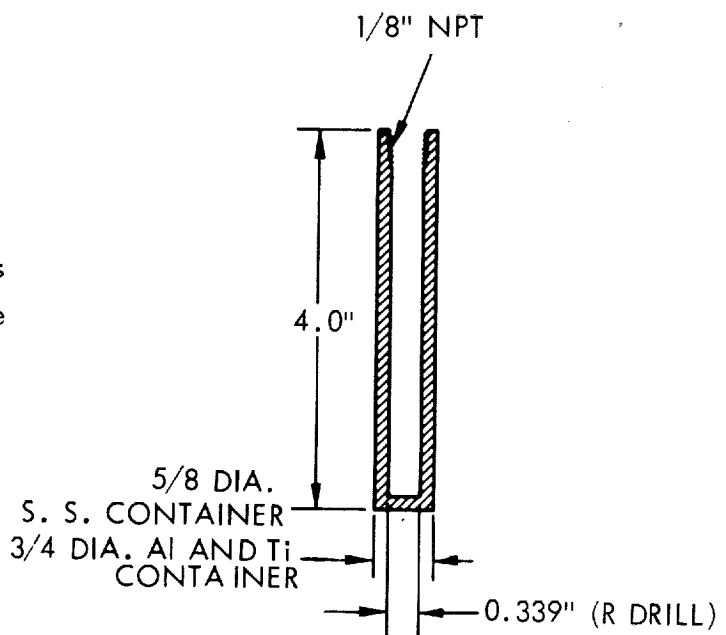


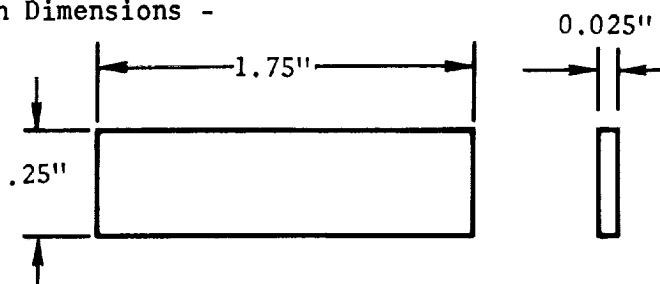
Figure 2-2. Configuration of Storage Container

Table 2-1. Corrosion Test Specimens

The pertinent physical data of the specimens, storage containers, and oxides are given in the following:

I. METAL SPECIMENS AND STORAGE CONTAINERS

- Volume of Propellants
 - 1.2 cc B_2H_6 at $-78^\circ C$
 - 1.5 cc OF_2 measured at $-196^\circ C$ (Stored at $-78^\circ C$)
- Total Volume of Storage Containers
 - 6 cc B_2H_6 Container
 - 6 cc OF_2 Container
- Percent Specimen Exposed to Liquid - 50%
- Percent Specimen Exposed to Vapor - 50%
- Specimen Dimensions -



- Specimen Surface Finish - Rolled mill sheet. The specimens and storage containers were cleaned in accordance with TRW Process Specification PR 2-3 as follows:
 - 6061-T6 Aluminum - Cleaned in 10% solution of Oakite Cleaner NST at $120^\circ + 20^\circ F$ for 15 minutes, followed by tap water and a distilled water rinse.
 - 347 Stainless Steel - Honed with 320 grit dry Alumina powder, washed in Alconox, then rinsed in tap water. This procedure is followed by a cleaning in accordance with TRW Process Specification PR2-9A, which uses Turco Vitro-Klene with Turco No. 4215 additive.
 - Ti-6Al-4V Alloy - The specimens were scrubbed with Ajax Cleanser and rinsed in tap water. This procedure is followed by a cleaning in accordance with TRW Process Specification PR2-17, which uses Turco HTC as the cleaning agent.

II. OXIDES OF STAINLESS STEEL

- Volume of Oxides - Approximately 2 cc
- Volume of B_2H_6 - 2 cc

2.3.4 Corrosion Specimens

The corrosion specimens were prepared and cleaned to the schedule reported in Table 2-1. The results of metallographic examination of representative samples in the "as received" condition were used to establish a baseline comparison with the specimens after storage.

2.4 TEST PROCEDURES

The containers were filled sufficiently to immerse half of the specimens in liquid propellant. The procedure used for loading and storing was as follows:

1. Cleaned specimens were placed in the storage containers and sealed to the test bay manifold (Figure 2-1) with pipe threads lubricated and sealed with Teflon tape.
2. The apparatus was pressure tested and vacuum tested until leaks were eliminated.
3. Dopants and propellants were added in proper sequence depending on volatility, so that the reactants were not brought together at a temperature higher than the storage temperature of -78°C .
4. Propellant was added to cover approximately one-half of the test coupon. The propellant was allowed to reach equilibrium vapor pressure at -78°C .
5. The propellants and test coupons were stored for 45 days prior to removal of the propellant for analyses and characterization of the liquid state.
6. Non-volatile residues and test specimens remaining in the storage containers were submitted for metallographic analyses.

2.5 METALLURGICAL EXAMINATION OF SPECIMENS

The metal specimens stored in doped oxygen difluoride and neat diborane were examined metallurgically. The examination consisted of measuring and weighing the pre and post tested samples, visual and photographic examination of the surfaces of the "post test" samples, and metallographic analyses of the longitudinal and transverse cross-sections of the samples for evidence of corrosive action of the propellants on the metal specimens. Table 2-2 outlines the results of the changes in thickness and weight, as well as the visual observation of the appearance of the surfaces. Figures 2-3a through 2-3f show the original longitudinal and transverse surfaces of the specimens, and Figures 2-4 through 2-7 show the changes in the surface structure of the samples.

Following is a detailed description of the results.

1. 6061-T6 Aluminum

The aluminum specimen exposed to diborane had a brighter surface after storage, and exhibited minor pitting in both the longitudinal and transverse direction.

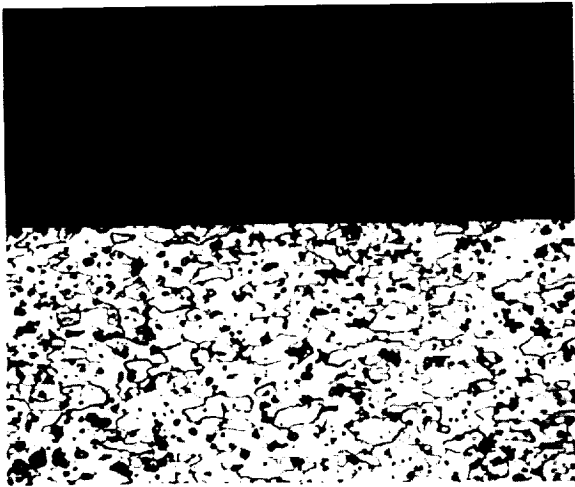
The aluminum specimen exposed to the doped OF_2 and stored in the aluminum bomb exhibited a slightly brighter surface and some pitting, which appeared to be more uniform over the exposed surface. The larger pits measured about 0.0003-inch diameter x 0.0003-inch deep and represented about 10 percent of the total ($220/\text{in}^2$) pits. The aluminum specimen stored in the stainless steel bomb, however, was more severely pitted, particularly in the transverse section, and seemed to be concentrated in the rolling marks on the specimen. The total pitting approximated $430 \text{ pits}/\text{in}^2$ and about 40 percent of these were the larger pits measuring at least 0.0025-inch diameter x 0.0006-inch deep. It is not known if the change in the corrosion behavior and surface appearance of the two aluminum samples is due to galvanic coupling with the stainless steel bomb, or if there was an interaction between the corrosion products of the aluminum specimen and the stainless bomb.

Table 2-2. Results of Corrosivity Tests on Metal Specimens
With Oxygen Difluoride and Diborane Stored For
45 Days

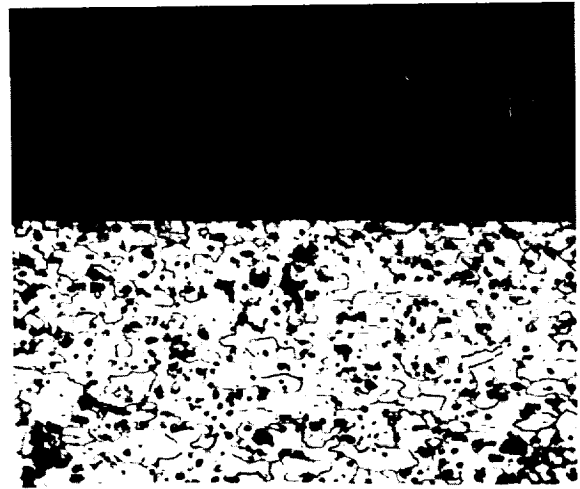
Material	Bomb	Propellant	Thickness Change, in.	Weight Change mg	Surface Appearance
Ti-6Al-4V	Ti-6Al-4V	B_2H_6^a	+ 0.0001	nil	Slightly brightened from control specimen
SS 347	SS 347	B_2H_6^a	- 0.0002	nil	Unaltered in appearance
Al 6061-T6	Al 6061-T6	B_2H_6^a	- 0.0004	-0.5	Surface brightened in appearance
Ti-6Al-4V	Ti-6Al-4V	OF_2^b	+ 0.0010	+2.9	Surface coated with orange- brown deposits, some evi- dence of pitting and surface darkening
SS 347	SS 347	OF_2^b	- 0.0001	nil	Surface slightly darkened
Al 6061-T6	Al 6061-T6	OF_2^b	- 0.0001	+0.6	Surface slightly brightened
Al 6061-T6	SS 347	OF_2^b	+ 0.0003	+0.2	Surface slightly darkened

^a B_2H_6 undoped

^b OF_2 doped with HF, O_2 , and H_2O



a. 6061-T6 Longitudinal View
(Original Magnification 200X)



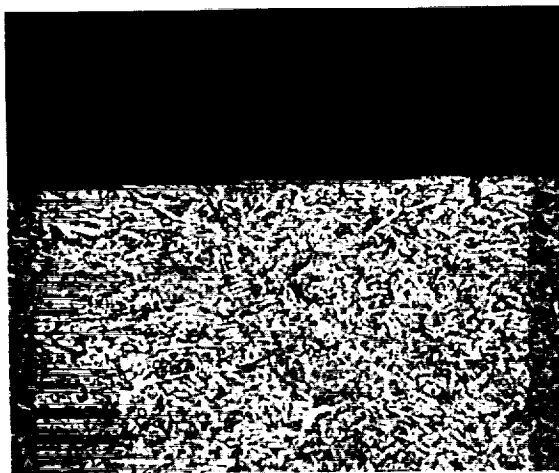
b. 6061-T6 Transverse View
(Original Magnification 200X)



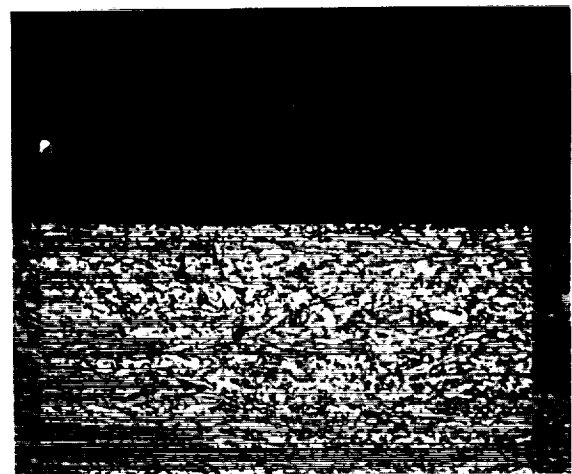
c. 347 SS Longitudinal View
(Original Magnification 200X)



d. 347 SS Transverse View
(Original Magnification 200X)



e. Titanium Alloy Longitudinal View
(Original Magnification 200X)

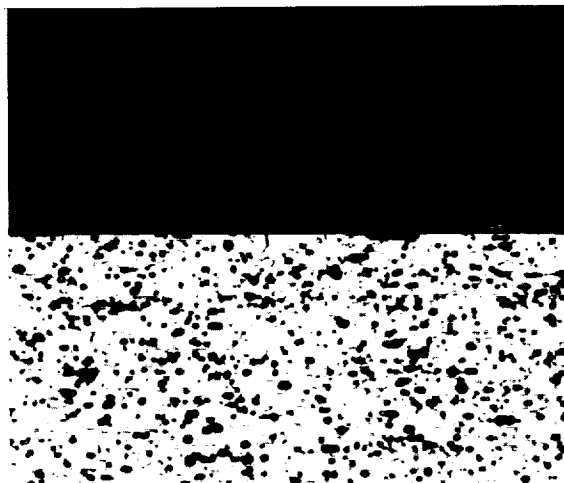


f. Titanium Alloy Transverse View
(Original Magnification 200X)

Figure 2-3. Comparison of the Longitudinal and Transverse Cross-Section of the Control Specimens Used in the Corrosion Tests



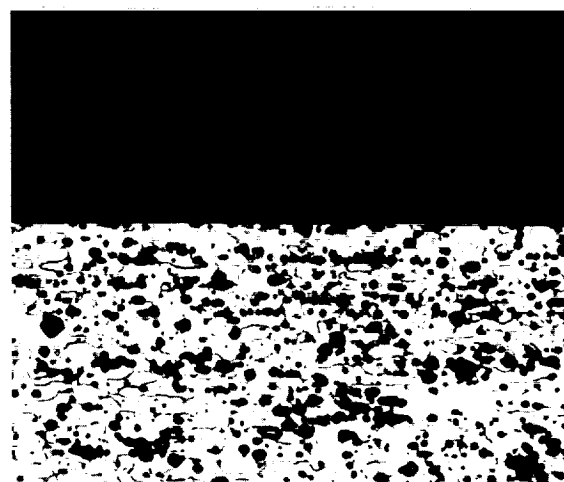
a. B_2H_6 Longitudinal Cross-Section
(Original Magnification 200X)



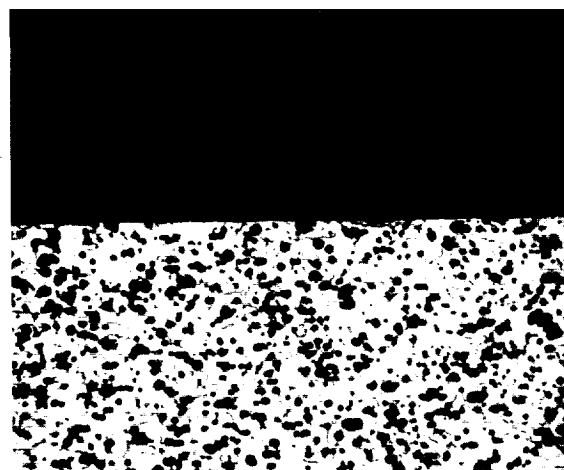
b. B_2H_6 Transverse Cross-Section
(Original Magnification 200X)



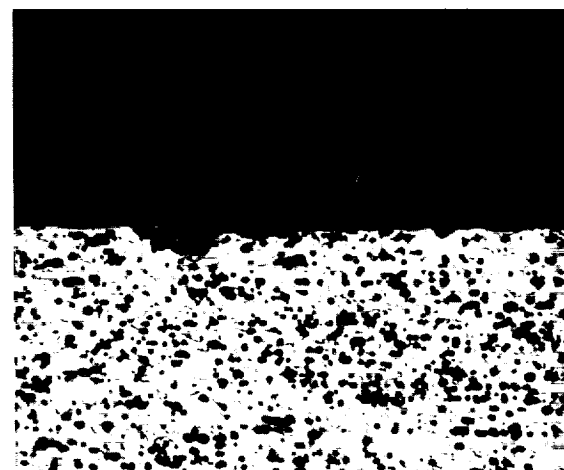
c. OF_2/Al Bomb Longitudinal Cross-Section
(Original Magnification 200X)



d. OF_2/Al Bomb Transverse Cross-Section
(Original Magnification 200X)



e. OF_2/SS Bomb Longitudinal Cross-Section
(Original Magnification 200X)



f. OF_2/SS Bomb Transverse Cross-Section
(Original Magnification 200X)

Figure 2-4. Comparison of the Corrosivity of Diborane and Oxygen Difluoride on 6061-T6 Aluminum Specimen

1. The first part of the document is a list of the names of the persons who have been appointed to the various positions of the Board of Directors of the Corporation.

2. The second part of the document is a list of the names of the persons who have been appointed to the various positions of the Board of Directors of the Corporation.

3. The third part of the document is a list of the names of the persons who have been appointed to the various positions of the Board of Directors of the Corporation.

4. The fourth part of the document is a list of the names of the persons who have been appointed to the various positions of the Board of Directors of the Corporation.

5. The fifth part of the document is a list of the names of the persons who have been appointed to the various positions of the Board of Directors of the Corporation.

6. The sixth part of the document is a list of the names of the persons who have been appointed to the various positions of the Board of Directors of the Corporation.

7. The seventh part of the document is a list of the names of the persons who have been appointed to the various positions of the Board of Directors of the Corporation.

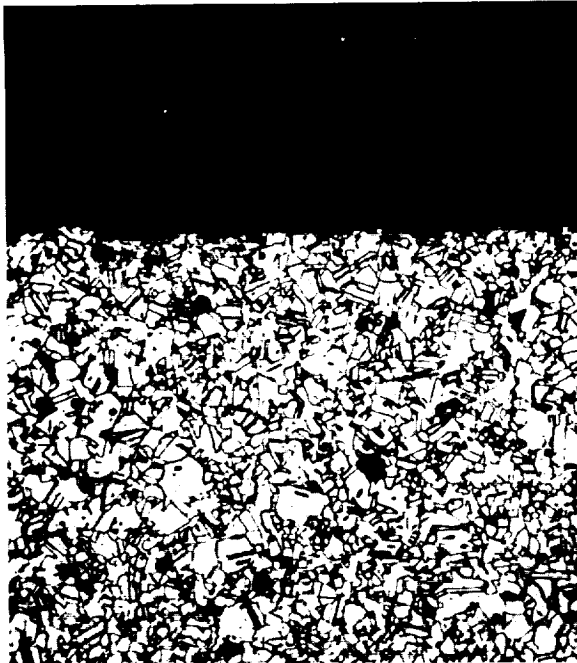
8. The eighth part of the document is a list of the names of the persons who have been appointed to the various positions of the Board of Directors of the Corporation.

9. The ninth part of the document is a list of the names of the persons who have been appointed to the various positions of the Board of Directors of the Corporation.

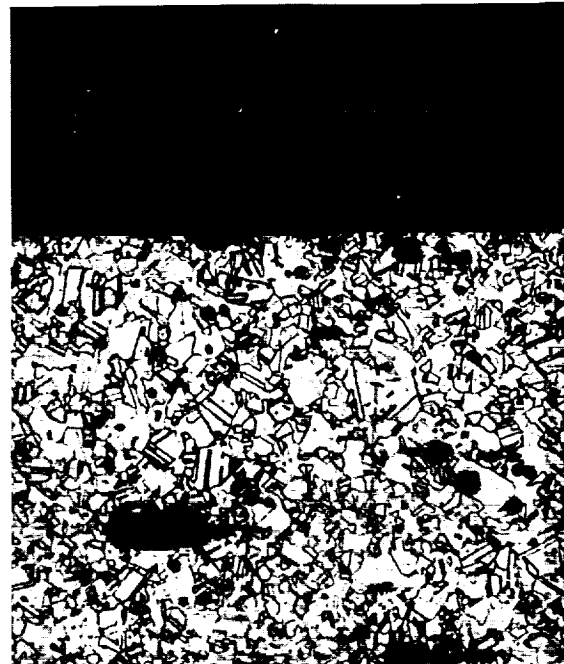
10. The tenth part of the document is a list of the names of the persons who have been appointed to the various positions of the Board of Directors of the Corporation.

11. The eleventh part of the document is a list of the names of the persons who have been appointed to the various positions of the Board of Directors of the Corporation.

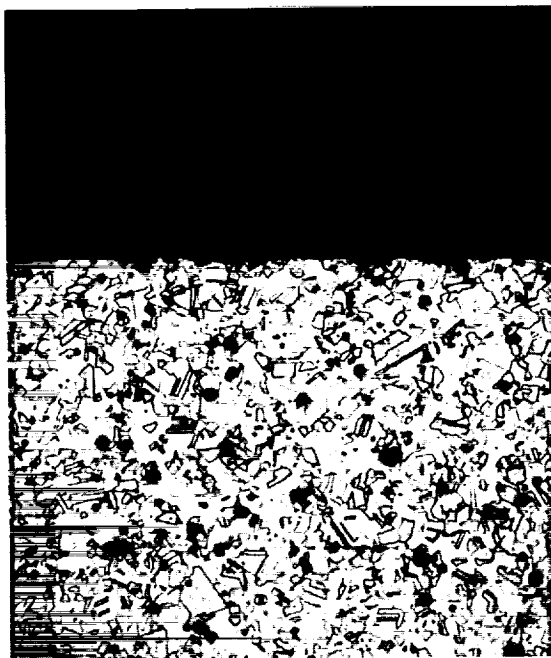
12. The twelfth part of the document is a list of the names of the persons who have been appointed to the various positions of the Board of Directors of the Corporation.



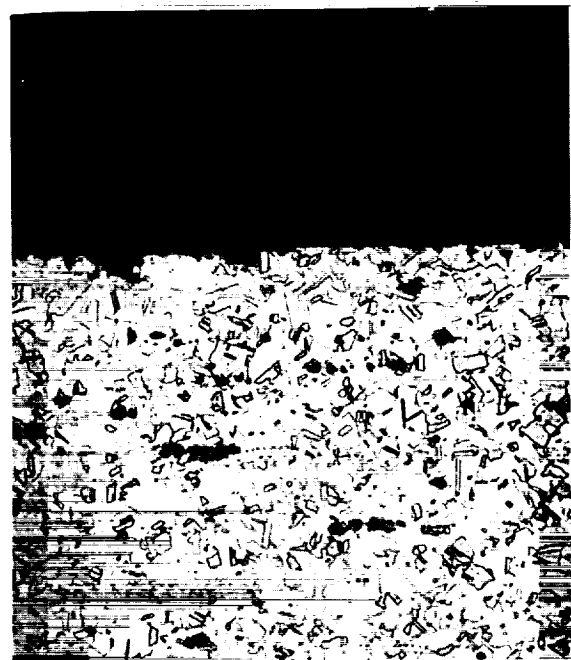
a. B_2H_6 Longitudinal Cross-Section
(Original Magnification 200X)



b. B_2H_6 Transverse Cross-Section
(Original Magnification 200X)



c. OF_2 Longitudinal Cross-Section
(Original Magnification 200X)



d. OF_2 Transverse Cross-Section
(Original Magnification 200X)

Figure 2-5. Comparison of the Corrosivity of Diborane and Oxygen Difluoride on 347 Stainless Steel Specimen

1. The first part of the document is a list of the names of the persons who have been appointed to the various offices of the Board of Directors of the Corporation.

2. The second part of the document is a list of the names of the persons who have been appointed to the various offices of the Board of Directors of the Corporation.

3. The third part of the document is a list of the names of the persons who have been appointed to the various offices of the Board of Directors of the Corporation.

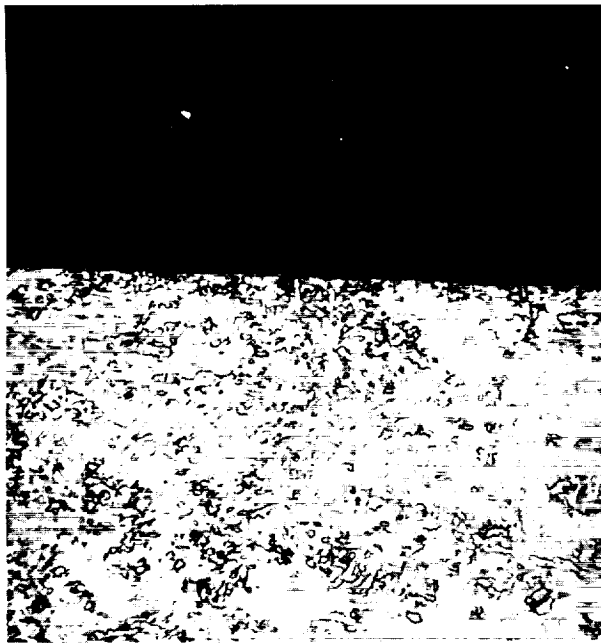
4. The fourth part of the document is a list of the names of the persons who have been appointed to the various offices of the Board of Directors of the Corporation.

5. The fifth part of the document is a list of the names of the persons who have been appointed to the various offices of the Board of Directors of the Corporation.

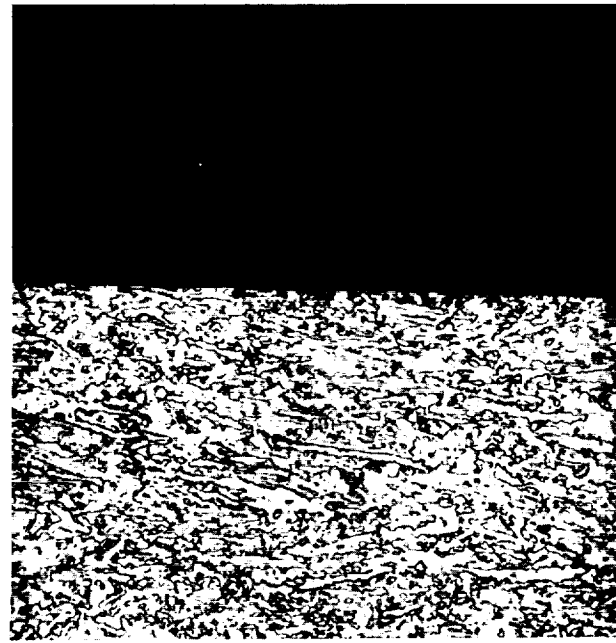
6. The sixth part of the document is a list of the names of the persons who have been appointed to the various offices of the Board of Directors of the Corporation.

7. The seventh part of the document is a list of the names of the persons who have been appointed to the various offices of the Board of Directors of the Corporation.

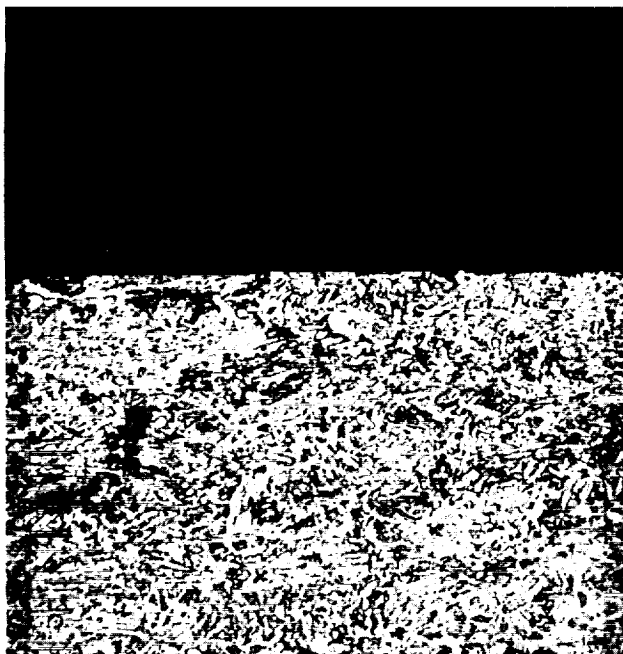
8. The eighth part of the document is a list of the names of the persons who have been appointed to the various offices of the Board of Directors of the Corporation.



a. B_2H_6 Longitudinal Cross-Section
(Original Magnification 200X)



b. B_2H_6 Transverse Cross-Section
(Original Magnification 200X)



c. OF_2 Longitudinal Cross-Section
(Original Magnification 200X)



d. OF_2 Transverse Cross-Section
(Original Magnification 200X)

Figure 2-6. Comparison of the Corrosivity of Diborane and Oxygen Difluoride on Titanium 6Al-4V Alloy Specimen

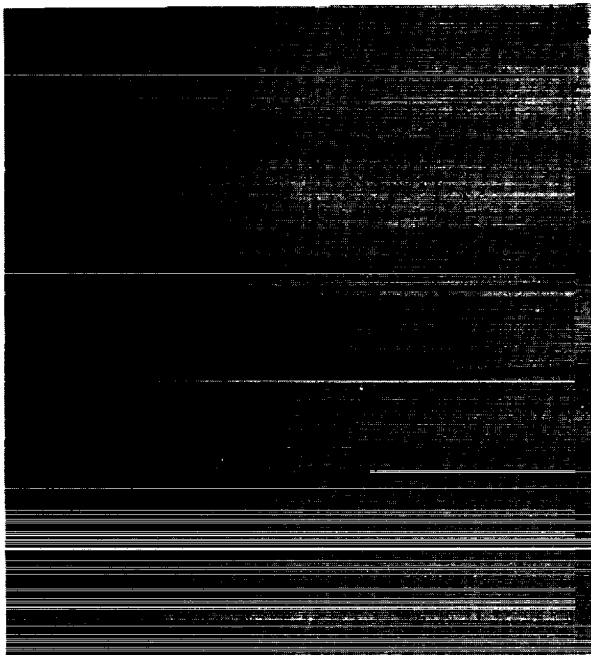
1. The first part of the document discusses the importance of maintaining accurate records of all transactions and activities. It emphasizes the need for transparency and accountability in financial reporting.

2. The second part of the document outlines the various methods and techniques used to collect and analyze data. It includes a detailed description of the experimental procedures and the statistical analysis performed.

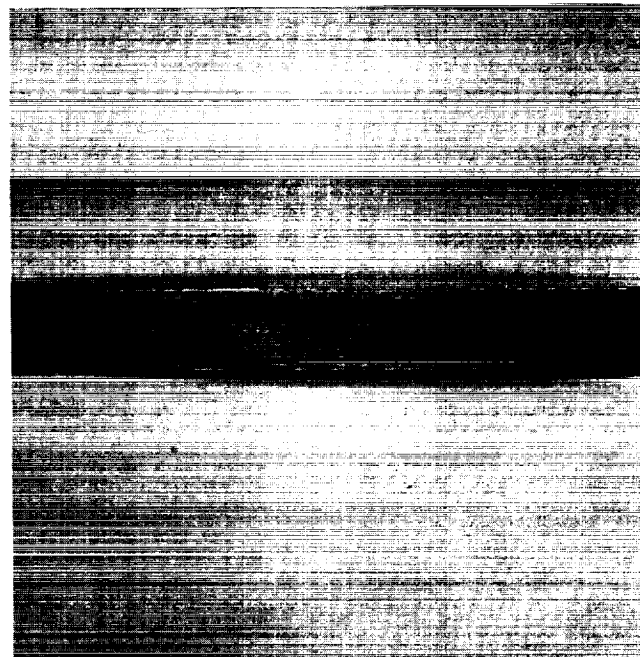
3. The third part of the document presents the results of the study. It includes a series of tables and graphs that illustrate the findings of the research. The data shows a clear trend of increasing activity over time.

4. The fourth part of the document discusses the implications of the findings. It suggests that the results have significant implications for the field of study and may lead to further research in this area.

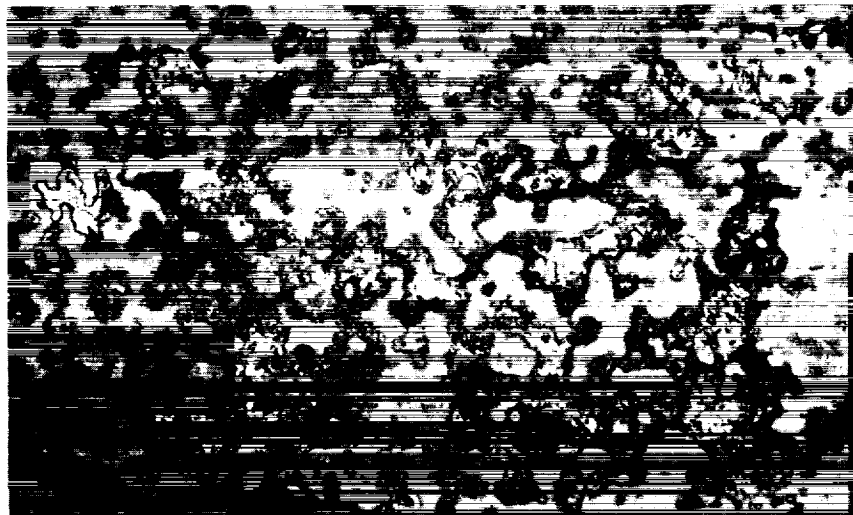
5. The fifth part of the document provides a conclusion and summarizes the key points of the study. It reiterates the importance of accurate record-keeping and the need for ongoing research in this field.



a. Control Specimen
(Original Magnification 1.5X)



b. Specimen Exposed to OF_2
(Original Magnification 1.5X)



c. Close-Up View of Surface Deposition
(Original Magnification 10X)

Figure 2-7. Comparison of Surface of Titanium 6Al-4V Control
with Specimen Exposed to Doped Oxygen Difluoride

2. 347 Stainless Steel

The stainless steel was relatively unaffected by the diborane, with only very minor pitting evident. The specimen exposed to oxygen difluoride showed slightly more pitting, although still relatively minor, and the surface was darkened slightly. Of the three alloys tested, the 347 stainless steel showed the least attack to either propellant.

3. Titanium-6Al-4V Alloy

Figure 2-6 shows the effect of OF_2 and B_2H_6 on the Ti-6Al-4V alloy. The diborane exhibited minimal attack on the alloy whereas the OF_2 specimen showed signs of pitting and, in addition, had an extensive deposit on the surface. This deposit is exhibited in Figure 2-7, which compares a control specimen to the specimen exposed to OF_2 . The deposit was extremely adherent, and some surface attack was evident under the deposit, as well as other pitting in areas which did not have the deposit present.

X-ray analyses were made on the area of the sample which had the deposit since there was an insufficient amount for a chemical analysis. Both diffractometry and powder pattern methods were utilized. The results indicated a high intensity of alpha phase titanium alloy, which was the base metal sample. Other constituents found included vanadium oxide (V_2O_5) and titanium oxides. The latter appears to be in the form of higher oxides of titanium such as Ti_4O_7 , but definite conclusions cannot be drawn due to the number of unassignable lines found.

4. Oxides of Series 304 Stainless Steel

The metal oxide samples were examined to determine if partial reduction of the oxide to metal had occurred, or if fine particles were present due to major morphological changes of the original oxide particles. Infrared spectrophotometric analyses of potassium bromide pellets of the original metal oxides and the conditioned

oxides showed no change due to the diborane. Visual and microscopic examination also indicated no obvious change. In an attempt to determine if minute morphological changes had occurred, both the original and conditioned oxides were examined with a Jealco Model JSM-2 scanning electron microscope. The scanning electron microscope has a depth of focus in the secondary electron mode that is several orders of magnitude greater than that available in any other type of microscope. This permits photomicrography of complex shapes with good clarity and sense of perspective. Figures 2-8a through 2-8d are scanning electron photomicrographs of the original and conditioned metal oxides, at a magnification of 3000X.

There appears to be slight changes in the surface structure of the oxides exposed to diborane, in that surface fissuring of the larger particles had occurred, and qualitatively, a larger number of smaller particles were present than in the unconditioned sample. Thus, some interaction had occurred between the diborane and the stainless steel metal oxides, but only to a relatively minor degree.

In order to verify if interaction had occurred between the diborane and the oxides of stainless steel, two more storage experiments were run. These experiments consisted of a repeat at -78°C for 30 days, and an accelerated test at -20°C for 30 days. Scanning electron microscopy was used as before to determine changes in surface morphology.

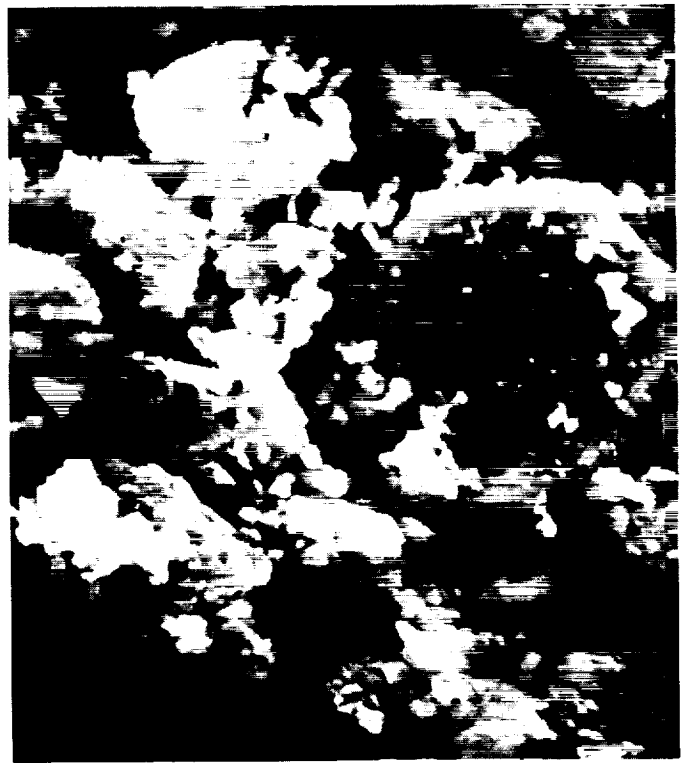
The repeat sample stored at -78°C showed essentially the same appearance as the previous sample: surface fissuring of the larger particles and a greater number of smaller particles, indicating sample breakup. Figures 2-8e through 2-8g show the sample. Due to considerable outgassing of the sample during the scanning mode, the photomicrographs at 3000X are not as clear as those taken previously. Figure 2-8g shows the sample at 1000X, which illustrates more clearly the larger amount of small sized particles present.

The sample stored at -20°C for 30 days showed considerable variation in general appearance. Approximately half of the sample was fused together, and considerable amounts of what appeared to be small metal particles were disseminated throughout the material. Figures 2-8h through 2-8j show the general appearance of the unfused portion of the material. Again, because of sample outgassing, the photomicrographs are not as clear as those taken previously. Figure 2-8j shows a portion of a metallic inclusion found in the powder. The general appearance of the unfused portion is a greater amount of surface fissuring, with about as many smaller particles as before.

Figures 2-8k and 2-8l show the appearance of the fused portion of the sample stored at -20°C for 30 days. Figure 2-9 is a photomicrograph of the entire fused chip, with the metallic inclusions clearly visible on the surface. The scanning electron photomicrographs (Figures 2-8k and 2-8l) show that the oxide particles have fused together into a laminar or foliated structure with no clearly discernable grain boundaries.



a. Untreated Powder (-325 mesh)
(Original Magnification: 3000X)



b. Untreated Powder (-325 mesh)
(Original Magnification: 3000X)

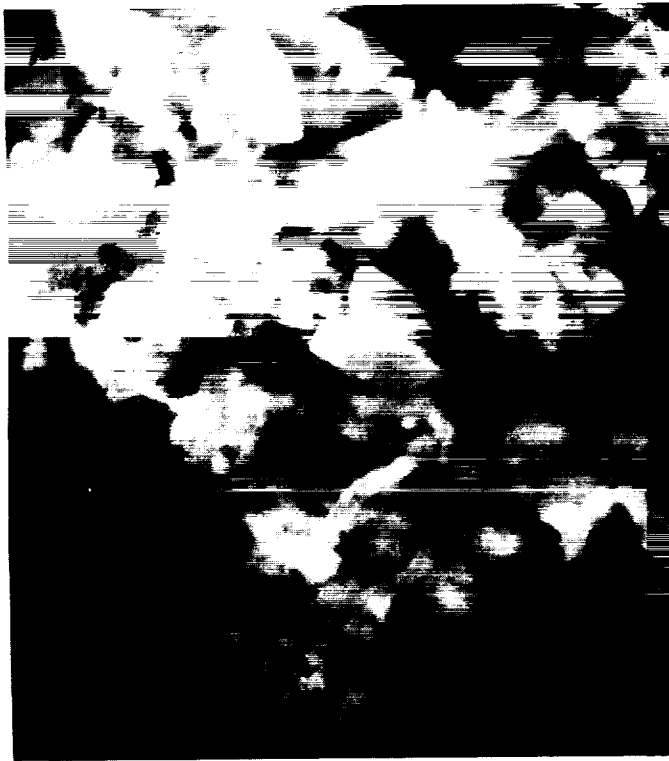


c. Powder (-325 mesh) in Contact
with B_2H_6 - 100°F for 45 days
(Original Magnification: 3000X)

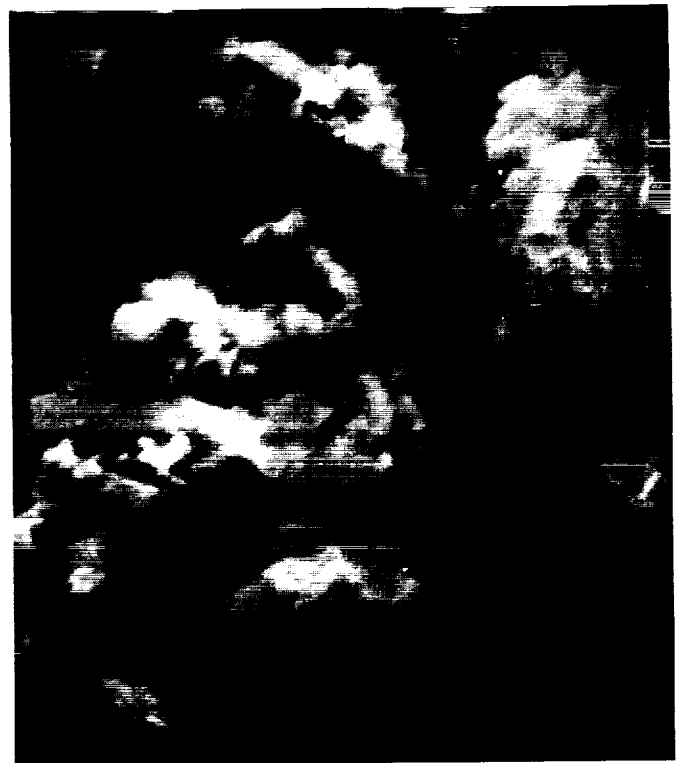


d. Powder (-325 mesh) in Contact
with B_2H_6 - 100°F for 45 days
(Original Magnification: 3000X)

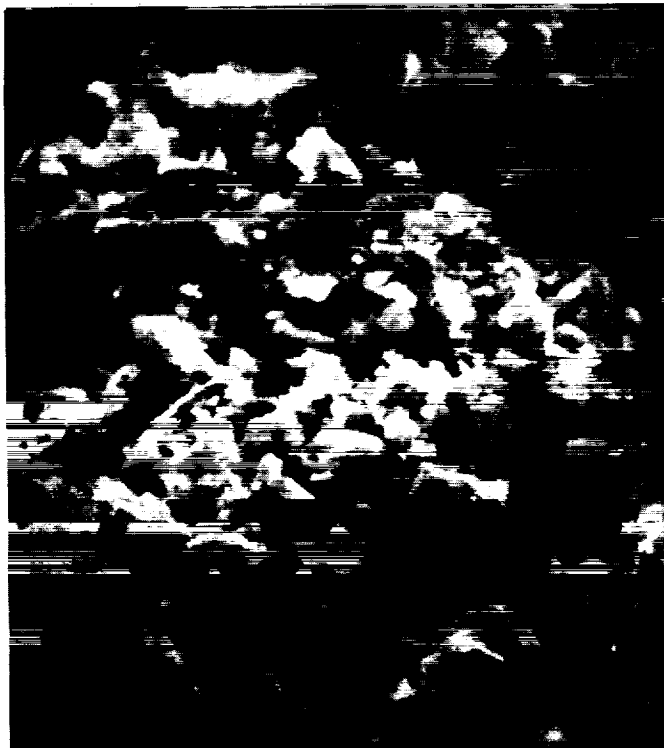
Figure 2-8. Scanning Electron Photomicrographs of
304 Stainless Steel Oxide Powder



e. Powder (-325 mesh) in Contact with B_2H_6 - $-78^{\circ}C$ for 30 days (Original Magnification: 3000X)



f. Powder (-325 mesh) in Contact with B_2H_6 - $-78^{\circ}C$ for 30 days (Original Magnification: 3000X)



g. Powder (-325 mesh) in Contact with B_2H_6 - $-78^{\circ}C$ for 30 days (Original Magnification: 1000X)

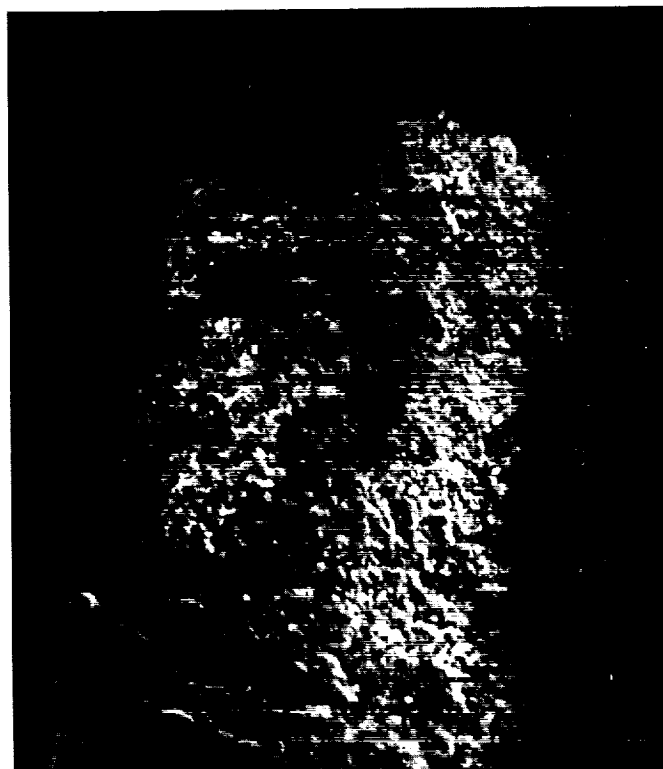


h. Powder (-325 mesh) in Contact with B_2H_6 - $-20^{\circ}C$ for 30 days (Original Magnification: 3000X)

Figure 2-8. Scanning Electron Photomicrographs of 304 Stainless Steel Oxide Powder - Continued



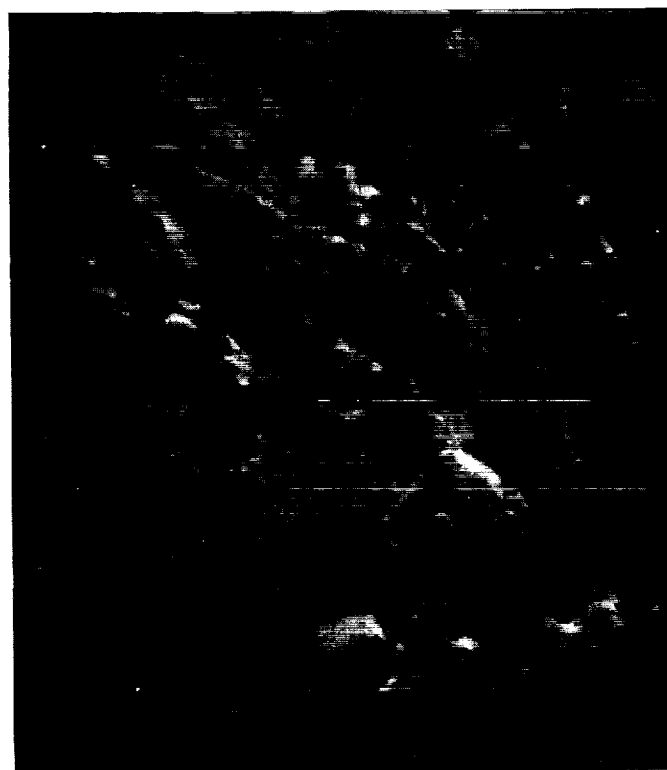
i. Powder (-325 mesh) in Contact with B_2H_6 - $-20^\circ C$ for 30 days
(Original Magnification: 3000X)



j. Powder (-325 mesh) in Contact with B_2H_6 - $-20^\circ C$ for 30 days
(Original Magnification: 100X)



k. Powder (-325 mesh) in Contact With B_2H_6 - $-20^\circ C$ for 30 days. Fused Chip
(Original Magnification: 100X)



l. Powder (-325 mesh) in Contact With B_2H_6 - $-20^\circ C$ for 30 days. Fused Chip
(Original Magnification: 1000X)

Figure 2-8. Scanning Electron Photomicrographs of 304
Stainless Steel Oxide Powder - Continued



Figure 2-9. Photomicrograph of Stainless Steel Oxides (-325 mesh). Exposed to Diborane for 30 Days. Fused Chip Portion (Original Magnification: 8X)

3.0 CHARACTERIZATION OF OXYGEN DIFLUORIDE AND DIBORANE (TASK 2)

3.1 INTRODUCTION

The purpose of this task was to characterize the propellants OF_2 and B_2H_6 in support of the corrosion study performed under Task 1 and to determine the effect of the corrosion of those selected metals on the chemical and physical properties of the propellants. Because of the inherent differences between the propellants, the samples stored in oxygen difluoride were analyzed by more indirect methods than were the samples stored in diborane. This was done because the oxygen difluoride is potentially more dangerous than diborane in metal and glass containers.

3.2 ANALYSES OF OF_2 AND B_2H_6

Because the propellants OF_2 and B_2H_6 are volatile, impurities are limited to materials, which are gases, at room temperature. Therefore, expanded gas samples of the propellants were analyzed by gas chromatography, infrared spectroscopy or mass spectrometry. It was not feasible to obtain analyses of oxygen difluoride by mass spectrometry (considered to be the best method) because of possible danger to the detector equipment, and the need for considerable preliminary passivation of the inlet system and auxiliary equipment for OF_2 use.

The propellants were analyzed for the presence of particulate matter after storage by examining them at temperatures near the storage temperature. The liquids were examined for evidence of, and changes in, Tyndall effect during temperature cycling by measuring the scattered light at right angles to the incident beam passing through the liquid. This testing determined if colloidal impurities were present or insoluble impurities were deposited during cycling. A laser light source was used in these studies to maximize detection sensitivity.

To prevent fractionation of the propellant during the analyses and to obtain representative samples of the liquid, the samples were either entirely evaporated and equilibrated in the gaseous phase (for OF_2 analyses), or the liquid phase was transferred (bled) directly into the analysis equipment

(for B_2H_6 analyses). Impurities of different volatility were not preferentially selected and analyzed by use of these methods.

3.2.1 Chemical Analyses of Oxygen Difluoride

Chemical analyses of oxygen difluoride were accomplished by gas chromatographic and infrared spectrophotometric techniques. Using gas chromatographic techniques, it was possible to determine oxygen difluoride, oxygen and carbon dioxide. Infrared analysis permitted determination of oxygen difluoride, silicone tetrafluoride, carbon tetrafluoride and carbon dioxide.

After termination of the 45-day storage period, the oxygen difluoride was removed from the storage container at the temperature of $-78^{\circ}C$, to prevent interference of the dopants, hydrogen fluoride and water. The oxygen difluoride and other volatile impurities listed above were distilled away, leaving the water and hydrogen fluoride in the storage containers with the metal test specimens. This step was important because the dopants and oxygen difluoride may react in an entirely different manner at room temperature or any intermediate temperature above $-78^{\circ}C$. Such corrosion might not be encountered during spacecraft storage. Later, any water and hydrogen fluoride or less volatile residues were removed by vacuum transfer from the test coupons as rapidly as possible while warming to prevent temperature induced chemical reactions. These dopants were examined by infrared spectrometry; the results are discussed later.

To obtain representative oxygen difluoride samples, the entire liquid sample was vacuum transferred to a liquid nitrogen cooled expansion bomb and later allowed to warm to room temperature in the closed expansion bomb. Samples were drawn from this bomb as needed for analyses. The expansion bomb developed about 90 psig at room temperature, making this a very convenient sampling device.

Results of the analyses showed no unusual change in impurity concentrations or new products except for an increase of oxygen in the oxygen difluoride.

Analyses of neat oxygen difluoride for oxygen by gas chromatography⁽¹⁾ using the conditions described below, indicates that the oxygen content in the neat oxygen difluoride is less than 0.5 percent, however, when the first sample is drawn into the vacuum transfer apparatus, analyses for oxygen may be as high as 1.0 percent. When the transfer apparatus becomes properly passivated with oxygen difluoride, the results of analyses of oxygen dropped below 0.5 percent and remained constant. The transfer apparatus was well passivated before being used in this study.

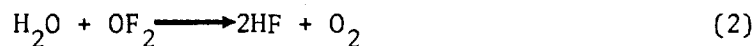
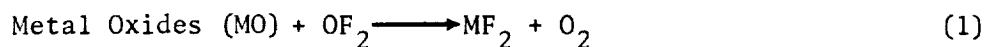
Gas Chromatography Operating Conditions Used
For Oxygen Analyses of OF₂ Propellant

Column	50 Percent Halocarbon Oil 4-11V on Kel-F 300 Powder
Length	30 feet
Diameter	1/4 inch
Carrier Gas	Helium
Flow Rate	30 cc/min
Temperature	25°C

The oxygen content in the propellant sample stored in the containers had increased to the level shown in the following table:

<u>Sample No.</u>	<u>Oxygen Content, % v/v</u>
347 SS	1.7
Ti 6Al-4V	3.3
Al 6061-T6	1.1
SS 347 Bomb	4.0
Al 6061-T6 Coupons	

Oxygen increase in the conditioning tubes could be attributed to either replacement of oxygen in metal oxides with fluorine atoms or the resultant of metal surfaces reacting with oxygen difluoride to release oxygen. Another source might be the reaction of oxygen difluoride with water to release oxygen. Possible reactions are:



Oxygen does not usually compete with fluorine in reactions with metals. This does suggest a potentially major problem in oxygen difluoride storage for long periods. Because oxygen is not a liquid at about -140°C , the temperature suggested for space storage, it must be determined whether oxygen continues to form. Oxygen is somewhat soluble in OF_2 , but -140°C is higher than the critical temperature of O_2 .

Using infrared spectrometry as the analytical tool, hydrogen fluoride dopant was observed to be partially recoverable except from the aluminum sample, but the water vapor was not recoverable. Water probably reacted according to equation (2). Complete recovery of hydrogen fluoride was not attempted nor would it be expected because much of it would remain adsorbed on the walls of the metallic vacuum system and valves even at very low pressure. Difficulty was encountered in loading the aluminum storage container with hydrogen fluoride dopant at -78°C . Hydrogen fluoride reacted to produce a non-condensable gas, probably hydrogen.

3.2.2 Chemical Analyses of Diborane

After storage at -78°C for 45 days, the storage container was removed from the storage area and transferred rapidly to a dry ice bath. The diborane samples were double valved and could be disconnected from the test manifold. One of the two valves and a sealant cap were warmed above room temperature to allow the connecting tube to dry. The sample was inverted and attached to the mass spectrometer inlet. The warm valve was opened and the system evacuated and leak tested. Later the chilled valve was opened slightly to allow liquid from the inverted sample to deliver a representative sample of the diborane into the mass spectrometer inlet system for analysis as previously discussed.

The sample was resealed and placed in storage again until it was later delivered to a viewing tube for laser examination.

Results of the mass spectrometer analyses, listed in Table 3-1, indicates that the original sample contained 0.79 percent hydrocarbons as butene and 0.64 percent isopropoxypentaborane. The concentration of these materials has been reduced in the test samples by the method of preparing the samples for storage. Partial fractionation was accomplished during the loading sequence because these impurities are less volatile than diborane.

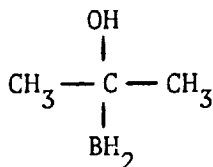
Table 3-1. Mass Spectrometer Analyses of Diborane

Constituent	Neat** Callery Chemical Diborane	Diborane in Contact With		
		6061-T6 Aluminum	347 SS	6Al-4V Titanium
Hydrogen	3.63	0.18	1.81	0.47
Diborane	94.53	98.87	97.59	98.44
Nitrogen	0.31	0.28	0.25	0.16
Oxygen	0.00	0.04	0.02	0.05
Hydrocarbons as (Butene)*	0.79	0.23	0.17	0.26
Carbon Dioxide	0.10	0.07	0.07	---
Isopropoxypentaborane	0.64	0.23	0.09	0.09

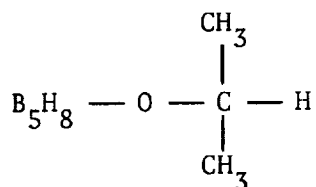
*The hydrocarbons were reported as butene rather than identifying the individual hydrocarbon molecules; butenes are perhaps fragments of higher molecular weight hydrocarbons.

**Stored in deep freeze -20°C for one year.

The source of isopropoxypentaborane in diborane is unknown but may be from acetone, which adds to diborane forming



followed by subsequent further reaction with B_2H_6 to produce the more stable pentaborane derivative,



Three test specimens of diborane stored with stainless steel oxides and one control sample were evaluated. The test conditions are given below:

<u>Sample No.</u>	<u>Test Conditions</u>
1	Control* 45 Days at -78°C
2	45 days at -78°C
3	30 days at -78°C
4	30 days at -20°C

*Oxides of stainless steel without B_2H_6

A chemical analysis of sample 2 was not originally scheduled in the program. However, the results of the metallurgical analyses of the oxides of sample 2 had indicated evidence of granular changes in the oxides, therefore, further testing was initiated with samples 3 and 4. The propellants used in samples 3 and 4 were chemically analyzed for impurities and the results are depicted in Table 3-2.

Table 3-2. Mass Spectrometer Analyses of B_2H_6

<u>Constituent</u>	<u>Sample No. 3</u> <u>-20°C</u>	<u>Sample No. 4</u> <u>-78°C</u>
Hydrogen	4.24	1.60
Hydrocarbons as Butene	0.03	0.05
Diborane	97.5	98.35

These results show less impurities N_2 , O_2 and CO_2 and isopropoxypentaborane than B_2H_6 analyses, Table 3-1. These were removed by vacuum fractionation prior to preparing samples 3 and 4.

3.3 LASER EXAMINATION OF OF_2 AND B_2H_6

To determine if storage of the selected materials or if the propellants in the dopants added were suspended in the liquids or would precipitate during temperature cycling near the proposed space storage temperature range, the liquid was examined after storage for evidence of Tyndall effect. A light beam from a helium-neon laser was passed through the liquid and the scattered light measured at right angles to the incident beam. The purpose of this examination was to determine if these propellants might have potential clogging materials present.

The apparatus for viewing the propellants in the liquid state is shown in Figures 3-1 and 3-2. The electronic equipment array is shown in Figure 3-3. The laser viewing assembly, Figure 3-2, was constructed inside a large clear Dewar flask to serve as a cryostat. It contained a laser viewing tube prepared from 1/2-inch O.D. heavy wall Pyrex tubing having optical flat surfaces at 90 degrees to each other. One laser light pipe was attached to each optically flat face, one serving as the inlet from the laser source and the other as an outlet to the detector for measuring the scattered light.

Laser light pipes were held in place by rigid conduit tubing welded to a ring which encircled the Pyrex tube. This is shown in the photograph, Figure 3-2, but not in the diagram, Figure 3-1.

Cryostat temperature was controlled by liquid nitrogen coolant delivered on demand using thermocouple sensors. A high speed stirrer circulated the nitrogen coolant continuously to assure temperature control.

The assembly was constructed to permit either vacuum transfer of the propellant sample to the viewing tube, or direct loading by pouring the sample into the top as shown in Figure 3-1. The latter method was considered to be the best method for obtaining a true sample of the propellant and more likely to contain the non-volatile impurities. However, for glass apparatus, it was not safe to transfer the conditioning tube with the liquid OF_2 at -78°C because of the high vapor pressure, 415 psig, at this

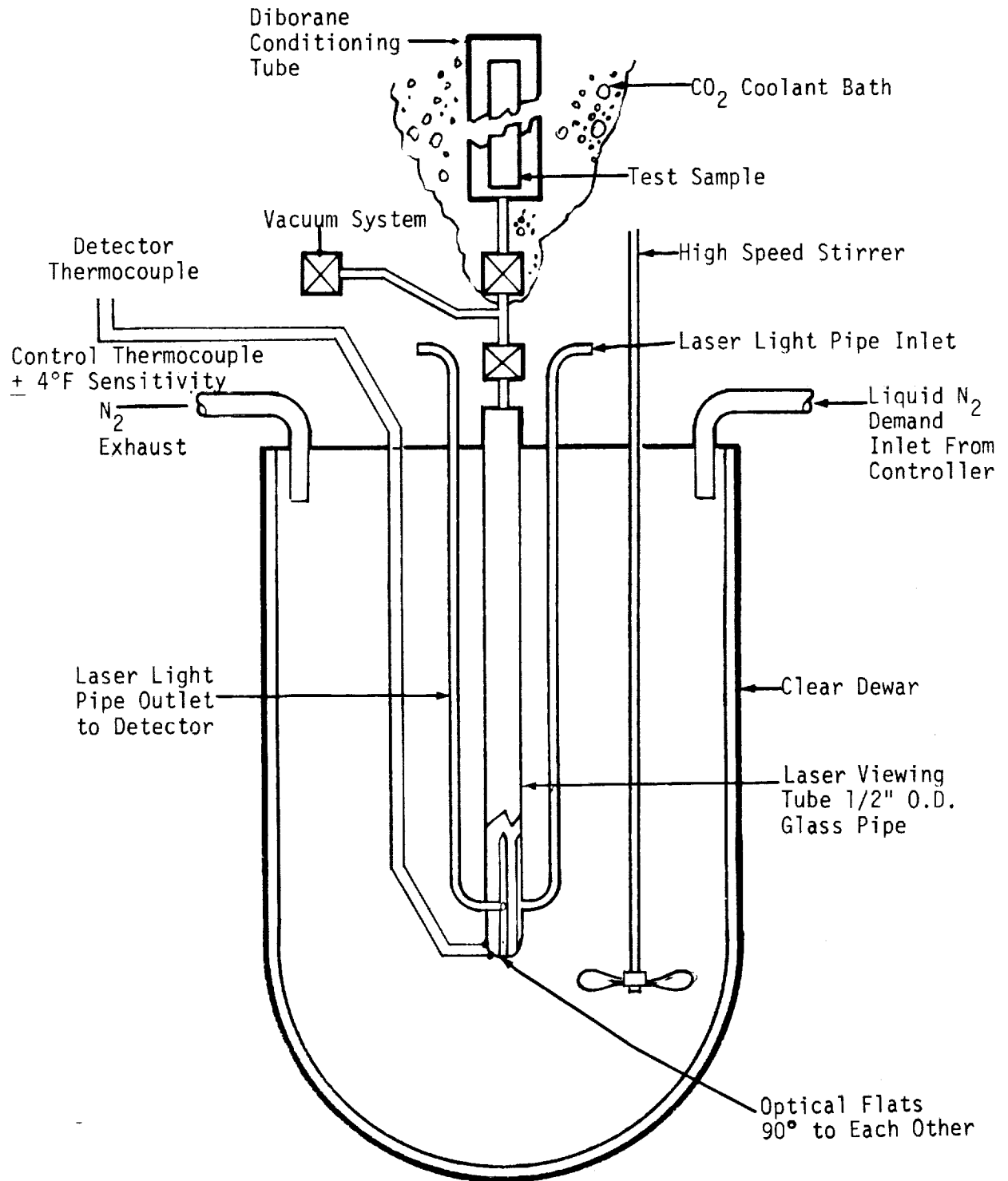


Figure 3-1. Laser Viewing Assembly

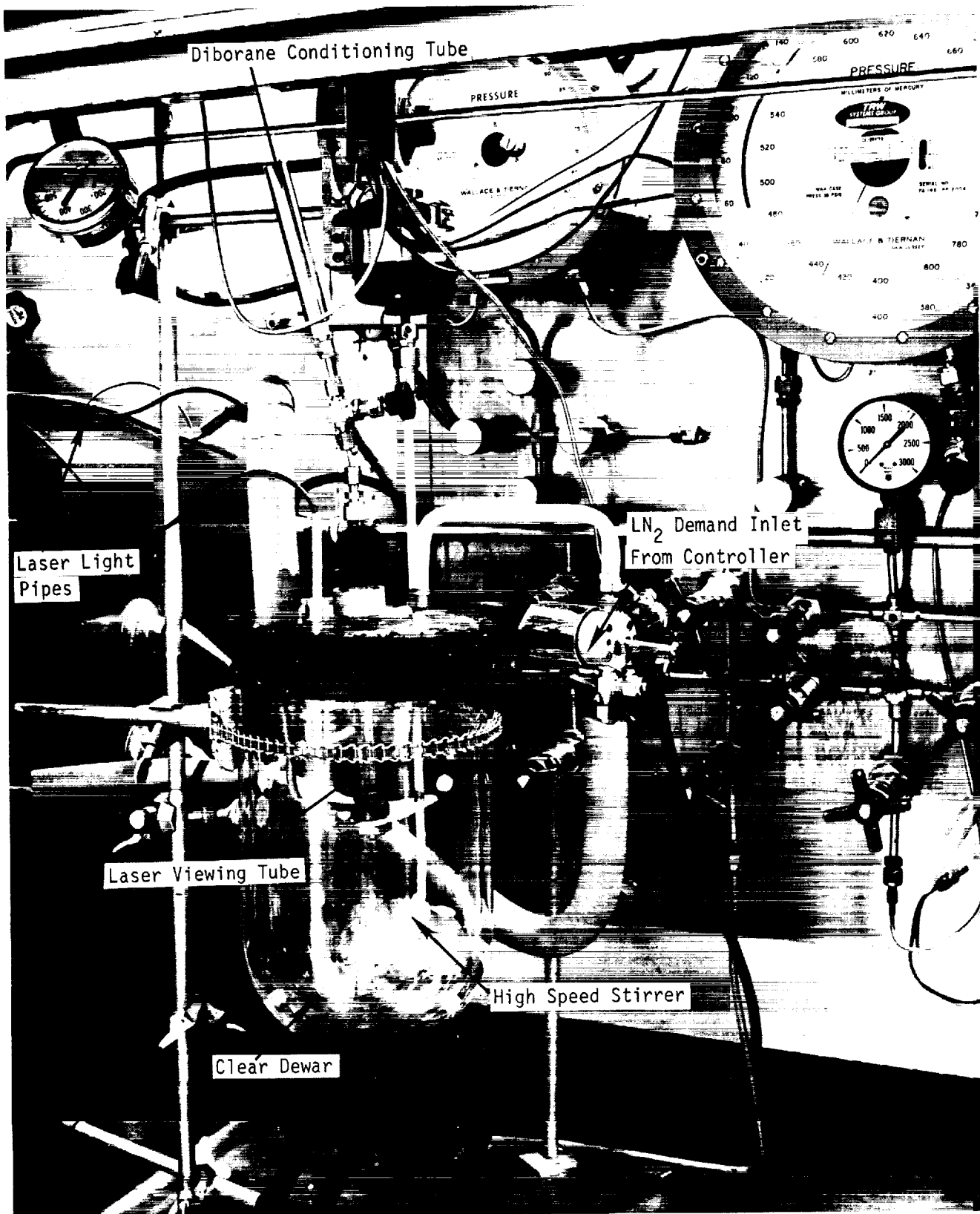


Figure 3-2. Photograph of Laser Viewing Assembly

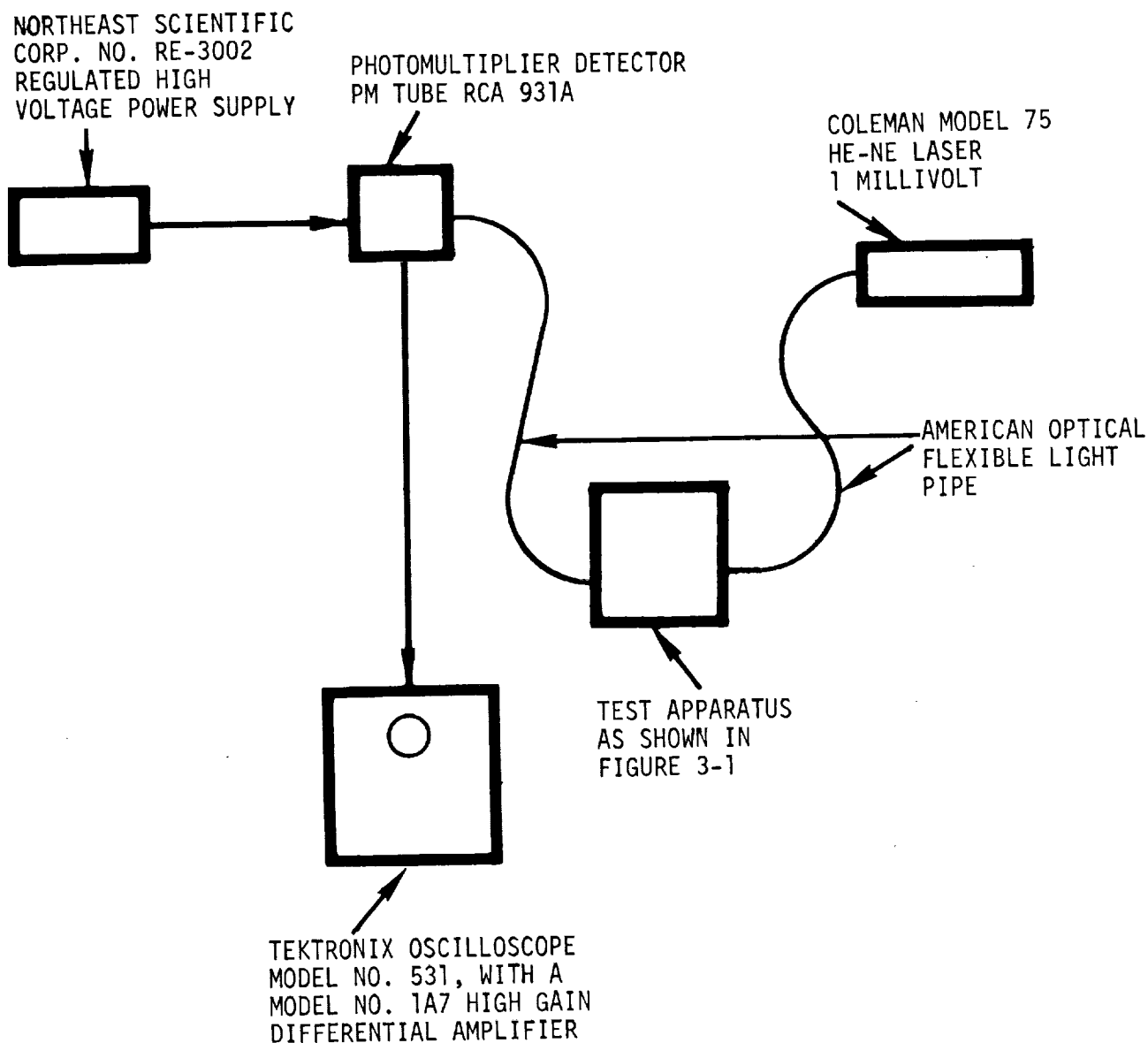


Figure 3-3. Apparatus for Detecting Tyndall Effect

temperature, and the probability that the glass or metal apparatus might ignite. Oxygen difluoride was vacuum transferred at a lower temperature and pressure for the study.

3.3.1 Laser Characterization of OF_2

Examination of the oxygen difluoride samples for the Tyndall effect at temperatures below -150°C with laser light was accomplished by transferring (evaporation and recondensation) the entire sample to the laser viewing tube, from the storage container. Because of the inherent danger

of transferring liquid OF_2 directly from an inverted sample bomb, all samples were condensed into the viewing tube from the vapor state. Thus, any material in solution in the OF_2 , unless volatile, was not present in the viewing tube. Examination of the storage containers and test samples for evidence of non-volatile residues was the alternate method used.

The baseline output from the photomultiplier tube for all of the OF_2 samples at -150°C was $250\ \mu\text{V}$. No change in voltage was noticed in any of the OF_2 samples unless the temperature was suddenly increased by at least 20°C . At that point, voltage shifts of $500\ \mu\text{V}$ corresponding to an increase in light scattering was noted, indicating either sudden precipitation of material or formation of bubbles due to the rise of the vapor pressure of OF_2 . After equilization at the higher temperatures, the voltage would revert to the normal baseline ($250\ \mu\text{V}$), indicating that either the precipitate (possibly CO_2) had redissolved or settled, or that the bubbles had risen out of the laser light path. Results of the laser examination for determining a Tyndall effect showed that a transient turbidity developed as the liquid temperature rapidly increased. The turbidity was not permanent and was attributed either to partial evaporation of liquid at the surface which deposited crystals that redissolved or to transient bubble formation. The turbidity developed at each warming step, not on the cooling cycle. This suggests that bubbles may be partially responsible for the turbidity. Although it is not known at this time which phenomena was occurring, the formation of CO_2 , HF or SiF_4 "snow" and its subsequent resolution is favored, since the formation of a white ring of material was noted at the liquid-vapor interface during evaporation, and other experiments have shown the presence of "snow" in the OF_2 .

These impurities were shown in the previous work⁽¹⁾ to be of limited solubility in liquid OF_2 . Commercial OF_2 usually has these impurities in the amount necessary to saturate the liquid held at the normal boiling point of liquid N_2 . The appearance of "snow" indicates a problem if OF_2 is partially evaporated, thus concentrating these materials beyond their solubility limits.

3.3.2 Laser Characterization of B₂H₆

For observing the liquid and measuring the change in Tyndall effect at temperatures below -78°C, the sample was bled, as described in 3.2, into a chilled laser viewing tube, Figure 3-1. The laser output beam was guided into the glass viewing tube through a light pipe placed against an optical flat on the tube. The scattered light, at 90 degrees to the incident beam, was collimated from an optical flat into another light pipe and the output directed against the photomultiplier tube. The scattered light was recorded on an oscilloscope and the Tyndall effect recorded as a microvolt shift from the value obtained at the propellant condensation temperature. Figure 3-3 shows the monitoring and data acquisition apparatus.

Results of the visual and laser examination of diborane between -78°C and the freezing point demonstrated a Tyndall effect throughout the entire temperature range. The diborane samples were transferred directly into the viewing tube through a cooled line, thus allowing a total examination of the diborane from the corrosion bomb. Three samples were examined: neat B₂H₆, B₂H₆ in contact with the 6061-T6 aluminum alloy, and the B₂H₆ in contact with the 347 stainless steel alloy. There was insufficient sample of the B₂H₆ in contact with the titanium alloy due to a leaking valve to perform the Tyndall effect measurements.

The baseline voltage for all of the diborane samples at -85°C was the same, 300 μV. The voltage increased as the temperature was lowered, indicating precipitation of material, which was verified by visual observation. The largest shift occurred in all samples after freezing when the temperature was held at -174°C, and subsequent reliquification, which left suspended solids in the liquid B₂H₆. The largest shift occurred in the B₂H₆ exposed to the 6061-T6 aluminum alloy (1.75 mV). The next largest shift occurred in the B₂H₆ exposed to 347 stainless steel (1 mV), and the smallest shift was with the neat B₂H₆ (0.5 mV). This corresponds to the results of the metallurgical examination of the metal specimens, as shown in Section 2.0.

The cause of the observed Tyndall effect is unknown but may be from the two impurities, isopropoxypentaborane and hydrocarbons. These impurities may have frozen or formed two phases as the temperature was lowered. Another possible cause of the observed Tyndall effect may be from colloidal boric oxide or partially hydrolyzed diborane. Boric acid is believed to be practically insoluble in diborane, however, the solubilities of partially hydrolyzed boron hydrides are unknown.

REFERENCES

1. "Investigation of the Formation and Behavior of Clogging Material in Earth and Space Storable Propellants," TRW Systems Group, Interim Report 08113-6016-R000, October 1968.

4.0 PROPELLANT FLOW TESTING (TASK 3)

4.1 INTRODUCTION

The objective of this task was to investigate the potential production of clogging materials in propellants during flow through small constrictions. The propellants tested were oxygen difluoride, diborane and hydrazine. In all flow runs the constriction used was a capillary tube. A description of the test facilities and test results are presented in the following sections.

4.2 OXYGEN DIFLUORIDE/DIBORANE FLOW TESTS

4.2.1 Flow System

The flow system schematic is shown in Figure 4-1. A list of operating conditions and construction components is included in Table 4-1. A photograph of the portion of the apparatus in the environmental test chamber is shown in Figure 4-2.

The test chamber which contained the flow system was chilled with liquid nitrogen coolant from a manifold of several portable liquid nitrogen tanks of 110 liter capacity. Two twelve inch, high speed fans circulated the nitrogen coolant within the test chamber continuously to assure isothermal conditions. The nitrogen inlet sprayed the liquid nitrogen on the rotating fan blades to cause the liquid droplets to be dispersed. Manufacturers' specifications indicated a temperature control of $\pm 4^{\circ}\text{F}$.

All components were constructed of 300 series stainless steel (see Table 4-1) except for copper stem gaskets in the three remotely controlled diaphragm valves. Two pipe thread connections were lubricated with Teflon tape. Seats in the AN fittings were 305 stainless steel.

The apparatus was constructed to contain and flow as much as one liter or quart of liquid propellant (three pounds of OF_2 or one pound of B_2H_6). A test capillary was chosen which had a 100:1 ratio of length to internal diameter, 0.010-inch I.D. The internal diameter was verified by passing a 0.009-inch diameter wire through the capillary, whereas a 0.010-inch diameter would pass only partially through each end of the tube.

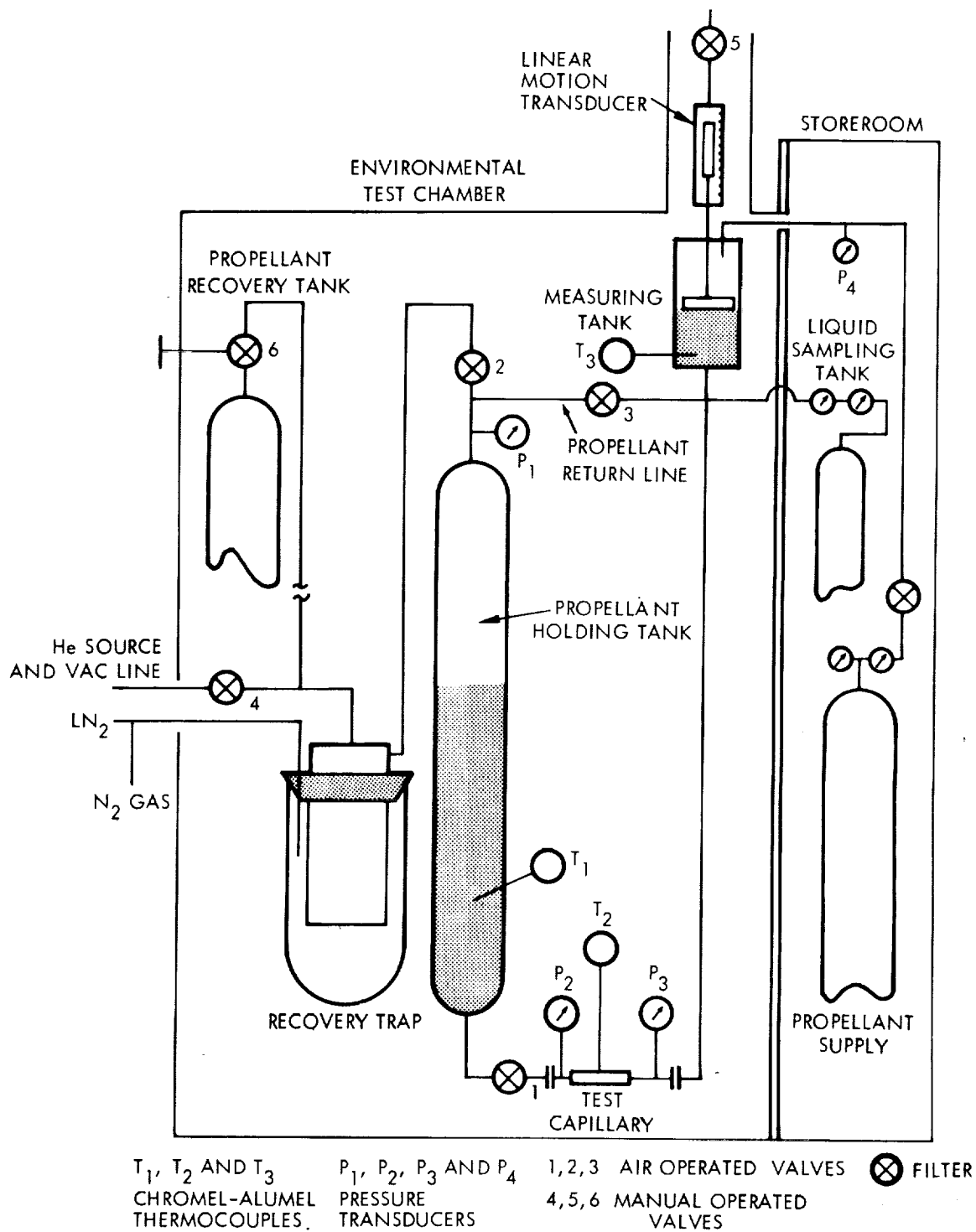


Figure 4-1. Schematic Diagram of Test Facility for $\text{OF}_2/\text{B}_2\text{H}_6$ Flow System

Table 4-1. Operation Conditions and Construction
Components for Flow Decay Studies

Environmental Test Chamber Bemco Inc.	40 cu. ft. box
Temperature	-140°C
Expected Temperature Control	$\pm 4^\circ$ at -140°C
Test Capillary Dimensions	1 in. long, 0.010-inch I.D.
Pressurant Gas Range	100 - 250 psia
Pressurant Gas	Helium
Maximum Operating Pressure	2000 psi, 250 psi for measuring tank float
Propellant Holding Tank Capacity Material	1 liter 304 stainless steel
Measuring Tank Capacity Material	1.2 liters 304 stainless steel
Liquid Level Sensing Device	10 inch linear transducer, DC output, 0.1% accuracy, G. L. Collins Corp., Long Beach
Remote Control Valve	1/4 in. Hoke 477 series bellows valve; copper seats
Hand Operated Valves	Hoke 4214 bellows valve; 305 stainless steel seats
Tubing	304 series 1/4 in. x .028 in. wall, 304 stainless steel AN fittings
Filters	1/2 in. AN fitting in-line filters, wire mesh 316 stainless steel
Pressure Transducers	Taber Teledyne, N. Tonawanda, N. Y. 0-300 psi range, Model 254

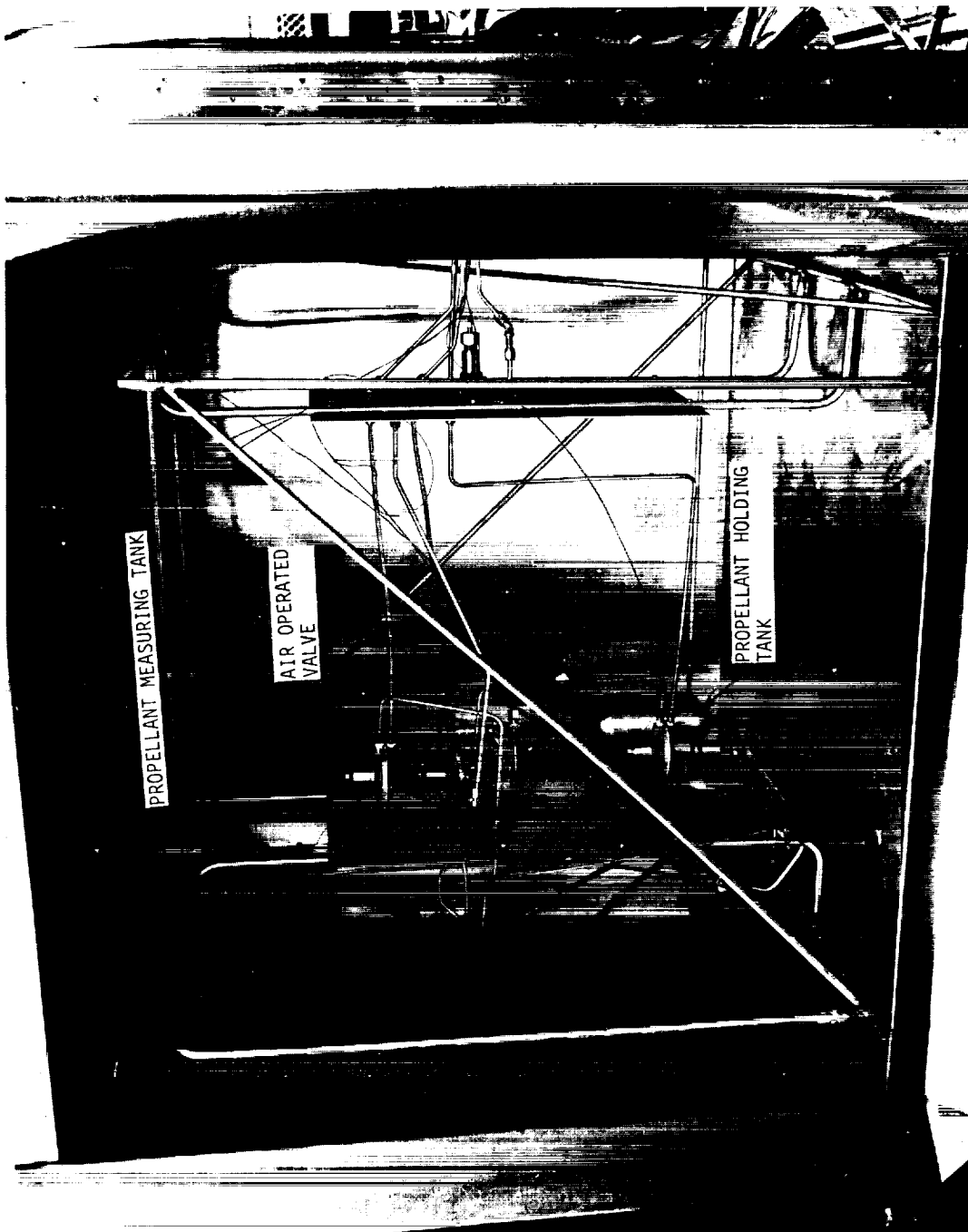


Figure 4-2. OF_2 Diborane Test Assembly

1. The first part of the document is a list of the names of the persons who have been appointed to the various positions of the Board of Directors of the Corporation.

2. The second part of the document is a list of the names of the persons who have been appointed to the various positions of the Board of Directors of the Corporation.

3. The third part of the document is a list of the names of the persons who have been appointed to the various positions of the Board of Directors of the Corporation.

4. The fourth part of the document is a list of the names of the persons who have been appointed to the various positions of the Board of Directors of the Corporation.

5. The fifth part of the document is a list of the names of the persons who have been appointed to the various positions of the Board of Directors of the Corporation.

6. The sixth part of the document is a list of the names of the persons who have been appointed to the various positions of the Board of Directors of the Corporation.

7. The seventh part of the document is a list of the names of the persons who have been appointed to the various positions of the Board of Directors of the Corporation.

8. The eighth part of the document is a list of the names of the persons who have been appointed to the various positions of the Board of Directors of the Corporation.

9. The ninth part of the document is a list of the names of the persons who have been appointed to the various positions of the Board of Directors of the Corporation.

10. The tenth part of the document is a list of the names of the persons who have been appointed to the various positions of the Board of Directors of the Corporation.

11. The eleventh part of the document is a list of the names of the persons who have been appointed to the various positions of the Board of Directors of the Corporation.

12. The twelfth part of the document is a list of the names of the persons who have been appointed to the various positions of the Board of Directors of the Corporation.

13. The thirteenth part of the document is a list of the names of the persons who have been appointed to the various positions of the Board of Directors of the Corporation.

14. The fourteenth part of the document is a list of the names of the persons who have been appointed to the various positions of the Board of Directors of the Corporation.

15. The fifteenth part of the document is a list of the names of the persons who have been appointed to the various positions of the Board of Directors of the Corporation.

Propellant from the holding tank, Figure 4-1, was pressure fed using helium pressurant through the capillary into the measuring tank. The measuring tank housed a float having a linear transducer attached to the top which determined the position of the float. The transducer would not operate at -140°C , the test temperature, and was therefore positioned outside the test chamber. By recording the position of this transducer during the flow experiments, the flow rate was determined.

The measuring tank was constructed of a 2.75-inch O.D. tubing, 0.065-inch wall, 16-inch long with welded caps having 1/4-inch tubing at the center for the propellant inlet and vent. A schematic diagram of this apparatus is shown in Figure 4-3. The propellant float was constructed of type 321 stainless steel tubing 2.50-inch O.D. by 0.020-inch wall, approximately 6 inches long. The ends were welded and walls reinforced with metal washers to permit use at 250 psig. Further reinforcement was accomplished by pressurizing the float with argon gas at about 150 psig.

The transducer probe was attached to the float with thin wall type 304 stainless steel tubing 0.108 inch O.D. Similar tubing was attached to the bottom of the float and extended down into the propellant delivery line from the test capillary. These tubes served as guides to prevent misalignment and fouling of the float against the wall.

The test capillary was constructed of type 304 stainless steel capillary tubing 1/16-inch O.D. by 0.010-inch I.D. and 1.0 inch long. The length to diameter aspect ratio was 100. A photograph of the capillary is shown in Figure 4-4. Figure 4-4 also shows the filters used in front of and downstream to the test capillary. The test capillary was heli-arc welded inside a 1/8-inch AN coupling having an internal diameter of slightly greater than 1/16 inch.

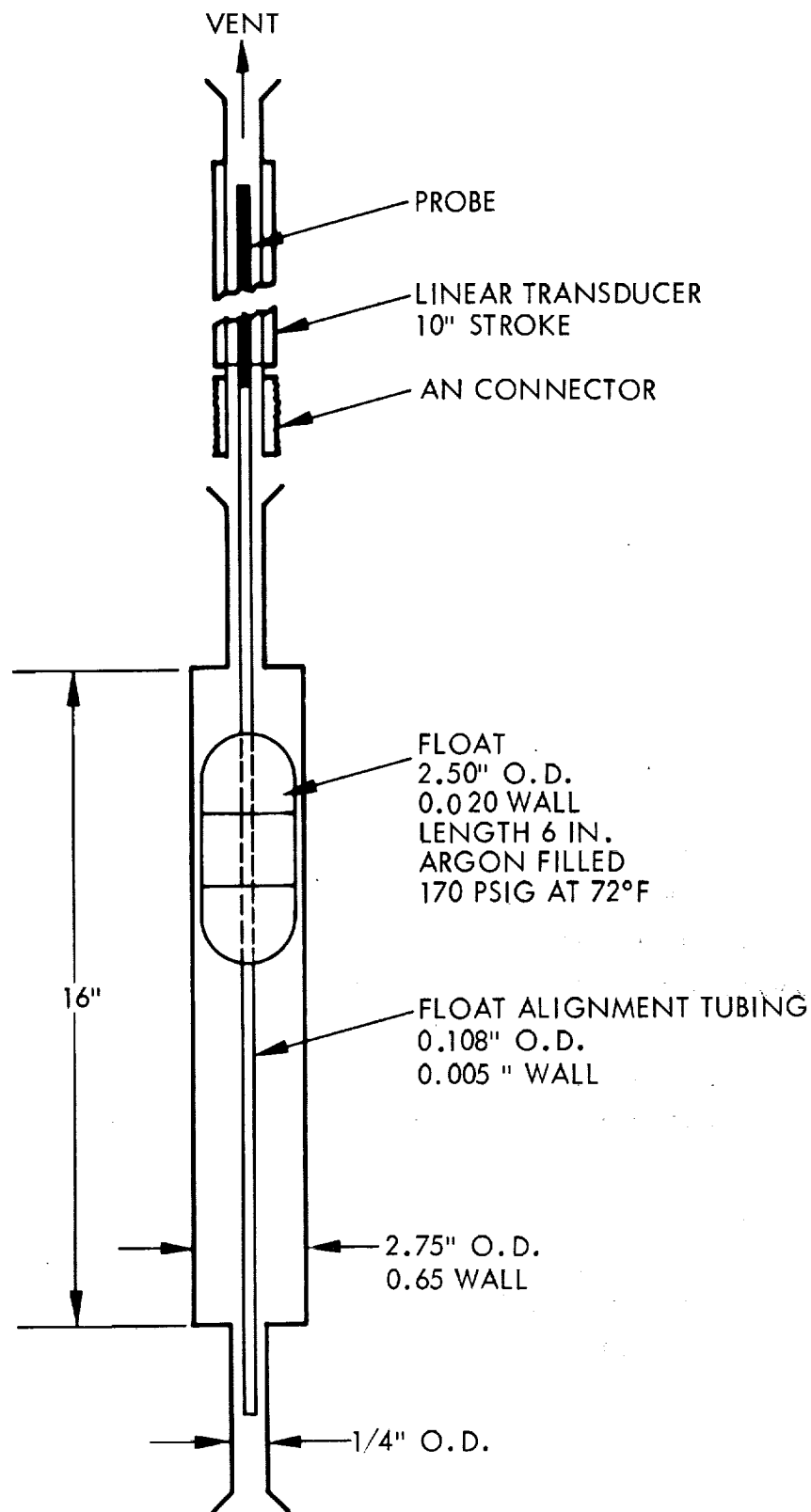
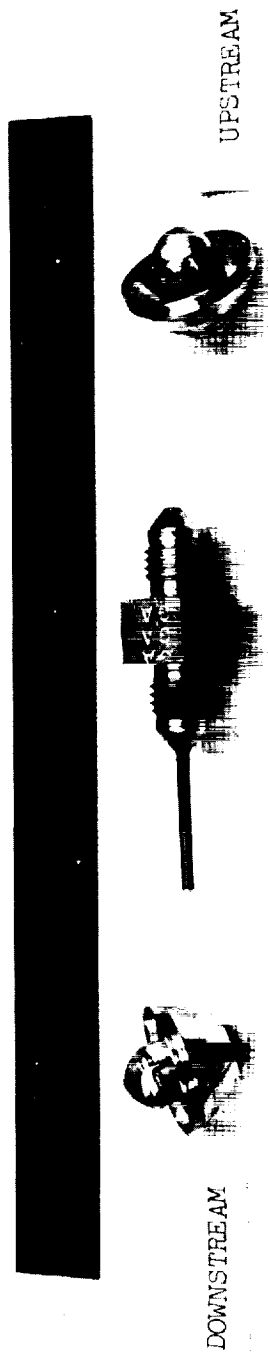


Figure 4-3. Flow Measuring Assembly



S/N S8-19310-5-1/2 MICRON RATING 5
WESTERN FILTER CO., GARDENA, CALIF.

S/N S8-19310-30-1/2 MICRON RATING 30
WESTERN FILTER CO., GARDENA, CALIF.

Figure 4-4. Photograph of Capillary Test Section and
Filters Used in $\text{OF}_2/\text{B}_2\text{H}_6$ Flow System

100

100

100

100

100

100

100

100

100

100

100

100

100

100

100

100

100

100

100

100

100

100

100

100

100

100

100

100

100

100

100

100

100

100

100

100

100

100

100

100

100

100

100

100

100

100

A thermowell was installed in the AN fitting near the capillary and a thermocouple was inserted to measure the capillary temperature.

Preliminary flow experiments using Freon and methyl alcohol were accomplished to verify the system performance.

4.2.2 Instrumentation

Instrumentation locations are shown on the schematic, Figure 4-5. The parameters monitored include temperatures, flow and pressure. The instrumentation techniques included the recording of all parameters on the Leeds and Northrup, Type W strip chart recorder with the exception of the float height which was recorded on the Hewlett Packard X-Y recorder. The temperature measurements were performed with Chromel-Alumel thermocouples with a 32°F reference junction temperature provided by an ice bath.

The temperature recording system was calibrated periodically with a thermocouple potentiometer to assure proper scale factor. The recorder scale was adjusted to indicate true temperature for operator convenience, but data reduction was performed with the thermoelectric voltage output to provide for the inherent non-linearities of thermocouples.

System component pressure measurements were performed with strain-gauge type transducers and signal conditioning units fed to the strip chart recorder. The pressure recording system was calibrated prior to most runs by resistance-pressure ("R-Cal") equivalents to set scale span and zero. "R-Cal" equivalents were determined from transducer calibrations performed by the TRW Systems Group Metrology Laboratory.

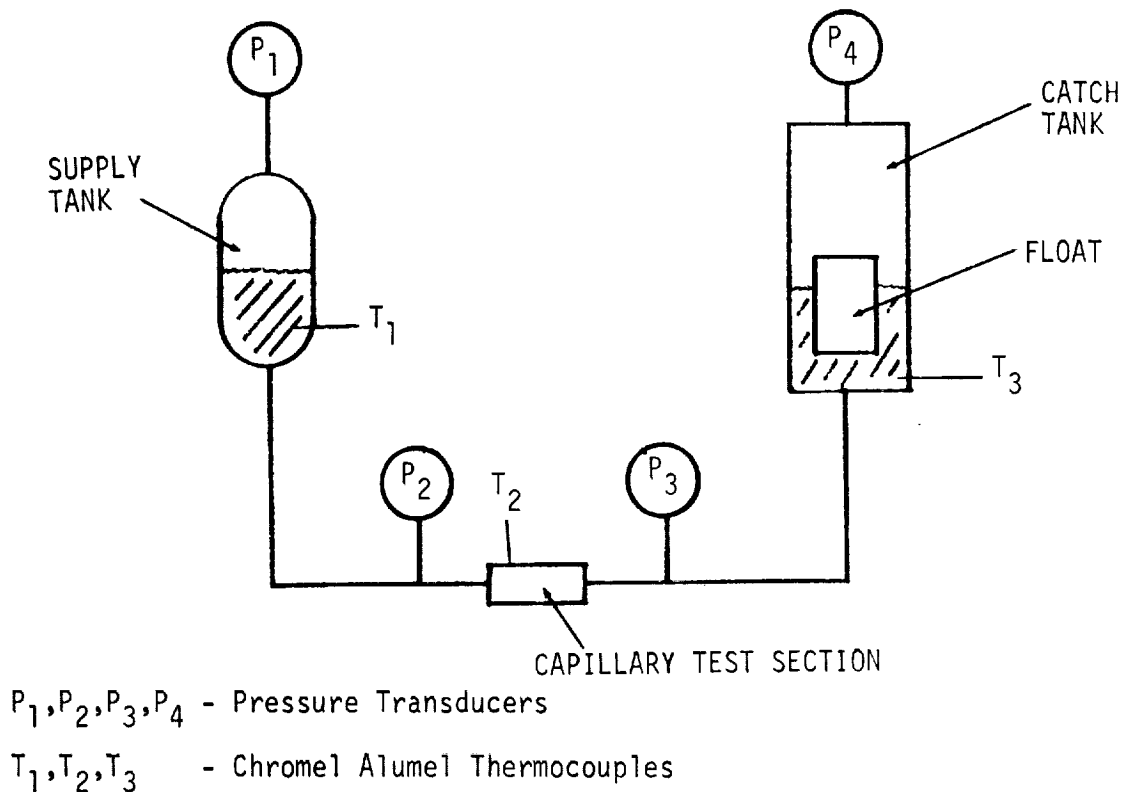


Figure 4-5. Transducer Placement on $\text{OF}_2/\text{B}_2\text{H}_6$ Flow System

Table 4-2 presents a tabulation of the worst case uncertainties in temperature, pressure, and flow measurements from run to run.

The "R-Cal" accuracy is a function of the calibration resistor tolerance and allows a constant systematic offset in pressure readout for any given resistor transducer pair.

The maximum within run measurement uncertainties are printed in Table 4-3. The measurement uncertainty is reduced considerably during steady state runs since the repeatability error of the instrumentation becomes negligible.

The uncertainties presented in Tables 4-2 and 4-3 were derived from data supplied by the TRW Metrology Department.

Table 4-2. System Measurement Accuracy Run to Run

Temperature

Thermocouple		$\pm 4.0^{\circ}\text{F}$
Recorder ($\pm 0.5\%$ of span, 300°F span)		$\pm 1.5^{\circ}\text{F}$
Reference Junction		$\pm 0.5^{\circ}\text{F}$
		<hr/>
		$\pm 6.0^{\circ}\text{F}$

Pressure

Transducer (linearity + repeatability)	$\pm 0.25\%$ F.S.	± 0.75 psi
Recorder	$\pm 0.5\%$	± 1.5 psi
R-Cal (accuracy of resistors used)	$\pm 0.15\%$	± 0.45 psi
	<hr/>	<hr/>
	$\pm 0.9\%$	± 2.7 psi

Flow	$\pm 2.3\%$
------	-------------

Table 4-3. System Measurement Accuracy Within a Single Run

Temperature

Thermocouple		$\pm 1.5^{\circ}\text{F}$
Recorder		$\pm 1.5^{\circ}\text{F}$
Reference Junction		
		<hr/>
		$\pm 3.0^{\circ}\text{F}$

Pressure

Transducer (repeatability)	$\pm 0.25\%$ F.S.	± 0.75 psi
Recorder	$\pm 0.5\%$	± 1.5 psi
	<hr/>	<hr/>
	$\pm 0.75\%$	± 2.25 psi

The instrument used for measuring the flow rate was a 10-inch D.C. output linear transducer having an inaccuracy of $\pm 1.0\%$ of the total range. This represents 0.1 inches inaccuracy of position in a measuring tank having an internal diameter of 2.6 inches and corresponds to a volume inaccuracy of 8 cc of liquid. The total free volume of the tank was about 1 liter.

4.2.3 Procedures and Operating Conditions

This section describes cleaning, testing and operation of the flow apparatus.

Cleaning and Leak Testing Procedures - A preliminary cleaning of the individual components included a Freon and acetone wash followed by high pressure dry nitrogen flush. Because of the danger of introducing small dirt particles from precleaned equipment, the apparatus was cleaned after assembly using the procedure outlined below:

1. Degreasing with Turco 3878 solution followed by distilled water rinse.
2. Ferratone wash followed by deionized water rinse.
3. Caviclean wash followed by deionized water rinse.
4. Alcohol wash (ethanol) followed by drying.
5. Freon wash with trichloro, trifluoro ethylene (Precision Cleaning Agent, NASA Specification 273-A).
6. Gaseous helium purge followed by pressure testing at 200 psig to locate large leaks.
7. Evacuation of volatile residues, with high vacuum apparatus.
8. Leak testing with helium leak detector.

During the above cleaning, all solutions were circulated for at least 15 minutes through all connecting lines and parts at a velocity of 10-20 times the flow velocity anticipated for the test flow condition. The test capillary was removed to allow more rapid flow through the lines. Several

filters were used in the circulating liquid to remove particles. The main filter was a Western Filter Co., Gardena, California, Model PN 19499-10, having a 10 micron filter element. During the Freon wash cycle, 100-ml samples of the circulating liquid were removed, under flow pressure, at several test orifices for cleanliness assay. These liquids were filtered through a Millipore filter and the residues examined with a microscope. When no particles above 100 microns were detected, the washing was completed.

Diborane was tested first. The cleaning procedure after B_2H_6 flow tests, prior to testing OF_2 , included an alcohol rinse, a dry nitrogen flush, followed by fluorine/oxygen passivation.

The fluorine passivation procedure included repeated pressurization of the apparatus with a fluorine/oxygen mixture (80% F_2 , 20% O_2), followed by complete evacuation of the system to less than 0.5 torr. Final passivation was done at 50 psig for 24 hours at room temperature.

Flow Testing and Operation of the Test Apparatus - Diborane was the first propellant tested because it is less corrosive to most metal parts than OF_2 . Diborane is a strong reducing agent and tends to convert air oxidized surfaces to partially reduce oxides or free metal. Reaction with water forms boric acid. The resultant hydride decomposition products are boron oxides or acids. These oxides and acids are readily removed with alcohol rinse which converts them to soluble and volatile borate esters. These esters were removed in the alcohol rinse.

Further removal of any boron residues was accomplished by the passivation process with a mixture of fluorine and oxygen which converts boron residues to volatile boron trifluoride.

Propellant was introduced into the environmental test chamber from the propellant supply tank. The test chamber was cooled to about $-140^\circ C$ to allow the propellant to liquify in the recovery trap or holding tank. The recovery trap served as an emergency tank which could be chilled directly from an independent liquid nitrogen source in the event of test chamber

malfunction. It would not be necessary to exhaust the propellant during such failure. The recovery trap also permitted more rapid cooling and heating of the propellant during transfer since it had an independent heating and cooling inlet line.

When the propellant holding tank was filled, valve No. 4 (see Figure 4-1) was opened to pressurize with helium gas. Valve No. 1 at the bottom of the holding tank was opened to permit the propellant to flow through the filter F_1 , test capillary, filter F_2 and to the measuring tank.

Flow rate was determined by continuously recording the position of linear transducer probe attached to the propellant float. Helium pressure on the propellant was reduced to the vacuum line through valve No. 4.

Propellant was returned by gravity flow through valve No. 3 or rapidly by pressurizing the propellant through valve No. 5 for repeat experiments.

Because OF_2 stored in contact with selected metals (see Paragraph 2.3.4) did not produce detectable quantities of contaminants, dopants were not added to the propellant before flow experiments were begun. Traces of impurities in the neat propellant assumed to be present were concentrated by partial fractionation of the propellant. After the completion of each experiment, the pressurant gas, helium, was vented which carried along with it a portion of the OF_2 , thus concentrating the impurities which were less volatile than the test propellant. All normal impurities, except oxygen, in OF_2 are less volatile than the propellant.

Impurities in OF_2 which would be expected to concentrate on partial evaporation of the liquid are hydrogen fluoride, silicon tetrafluoride, carbon tetrafluoride and carbon dioxide. Hydrocarbons and isopropoxy-pentaborane are impurities in diborane and are less volatile than diborane.

4.2.4 Propellant Sources

Propellants used for the flow experiments were manufactured by Allied Chemical Corporation (OF_2) and Callery Chemical Corporation (B_2H_6). Both samples were condensed from the manufacturers' supply tank to the flow apparatus. The diborane sample was delivered from the supplier in dry

ice coolant and stored at -20°C for one year prior to analyses. The mass spectrometric analysis of the neat diborane at the time of use is shown in Table 3-1.

4.2.5 Diborane Test Results

Diborane test results, runs 3 through 11, Table 4-4, showed no evidence of blockage or flow decay. There were no solid residues left on the filters after these experiments were terminated and the propellant removed from the system. In run No. 8, a decrease in flow rate from 20.6 cc/min to 14.0 cc/min could not be attributed to increase in pressure in the measuring tank. This was the only significant anomaly resulting from the series of flow runs.

The velocity of diborane through the 0.010-inch diameter capillary varied from approximately 22 ft/sec to 44 ft/sec for the range of flow rates from 20 cc/min to 40 cc/min, respectively. The calculated Reynolds number based on flow rates of 20 cc/min and 40 cc/min were 2600 and 5200, respectively. The low Reynolds numbers fall into the critical or transition zones on the Moody Diagram. The calculations were based on a kinematic viscosity of $7 \times 10^{-6} \text{ ft}^2/\text{sec}$.

Within the range of velocities, temperatures, and capillary size tested, it was concluded that neat diborane does not appreciably exhibit flow decay.

4.2.6 Oxygen Difluoride Test Results

Results of the flow tests are listed in Table 4-5, experiments 12 through 17. There was no evidence of blockage, flow decay or any unusual observations under the conditions studied. Flow rate changes were attributed to the changes in the pressure in the measuring tank due to decreasing free volume in the tank during flow. The velocity of the OF_2 propellant through the 0.010-inch diameter capillary ranged from 16 ft/sec to 32 ft/sec corresponding to flow rates from 15 cc/min to 30 cc/min. Reynolds numbers ranged from 6,600 to 13,200, indicative of flow in the transition to turbulent range. Examination of the capillary tube and the two filter elements upstream and downstream to the capillary with a microscope before and after the experiments revealed no unusual particles or evidence of erosion due to the tests.

Table 4-4. Diborane Test Results at -145°C
(Helium Pressurant)

Run No.*	Time Sec.	Pressure				Flow Rate cc/min
		Holding Tank P ₁ PSIG	Capillary		Measuring Tank P ₄ PSIG	
			Upstream P ₂ PSIG	Downstream P ₃ PSIG		
3	100	246	242	6	7	27.7
	200	245	242	0	0	29.4
	300	245	242	0	0	27.9
3A	100	99	96	0	0	19.2
	200	94	92	0	0	19.4
	300	92	88	0	0	19.6
4	100	236	232	0	2	31.1
	200	236	232	3	4	31.0
	300	236	232	6	3	31.0
	400	236	232	1	3	31.3
5	100	239	236	1	2	37.3
	200	239	235	4	5	36.8
	300	239	235	9	10	37.0
	400	239	235	14	16	36.8
6	100	238	235	10	10	34.6
	200	238	235	15	15	35.5
	300	238	235	11	11	34.8
	400	238	234	16	16	35.6
7	100	162	160	10	10	21.3
	200	161	160	12	12	21.0
	300	161	160	15	15	21.0
	400	161	160	9	9	21.3
	500	161	160	13	13	20.8
	600	161	159	16	16	20.5
8	100	101	99	3	3	20.1
	200	101	99	4	5	19.9
	300	100	99	6	6	20.1
	400	100	99	8	9	20.6
	500	100	99	10	11	14.0
	600	100	99	14	14	18.9
9	100	100	99	3	4	21.9
	200	99	98	5	5	21.3
	300	99	98	18	8	20.8
	400	99	98	10	10	20.6
10	100	176	174	3	3	29.4
	200	176	174	6	6	29.2
	300	176	174	9	9	28.9
	400	176	174	13	13	28.5
11	100	231	229	5	6	34.6
	200	231	228	9	9	35.1
	300	231	228	14	14	34.5

*Runs 1 & 2 Operational Test - V

*Runs 1 & 2 - Operational Tests, No Data Recorded

Table 4-5. Oxygen Difluoride Test Results at -145°C
(Helium Pressurant)

Run No.	Time Sec.	Pressure				Flow Rate cc/min
		Holding Tank P ₁ PSIG	Capillary		Measuring Tank P ₄ PSIG	
			Upstream P ₂ PSIG	Downstream P ₃ PSIG		
12	0	79	75	8	6	17.2
	120	79	75	9	8	16.5
	240	79	75	12	10	15.8
	360	79	74	14	12	15.7
	480	78	74	17	15	15.4
	600	78	74	18	16	14.8
	720	78	74	19	17	14.9
13	0	116	111	16	14	20.6
	120	116	111	19	17	20.0
	240	116	111	21	20	19.5
	360	115	111	26	24	19.1
	480	115	111	31	29	18.3
14	0	110	107	28	26	19.3
	120	110	107	22	21	19.1
	240	110	106	9	6	20.4
	360	110	106	11	10	19.5
	480	110	106	14	12	20.0
15	0	206	202	15	17	28.5
	100	206	202	19	21	27.1
	200	206	201	23	26	26.6
	300	206	201	29	30	25.7
	400	206	201	36	38	28.1
16 *	0	208	203	9	9	28.6
	100	207	203	12	12	27.4
	200	207	203	16	16	27.6
	300	207	202	18	18	26.8
17 *	0	225	222	6	6	30.2
	60	225	221	8	8	29.0
	120	225	221	9	9	29.7
	180	225	221	12	12	29.3
	240	225	221	14	14	28.5

*Oxygen Pressurant

4.3 HYDRAZINE FLOW TESTING

The objective of this portion of the study was to investigate potential flow clogging phenomena in liquid hydrazine. An extrusion rheometer was previously employed for the study of flow clogging phenomena with liquid hydrazine⁽¹⁾. The extrusion rheometer represents a less costly and simpler method for these studies than the full scale flow bench operation.

In this study, the rheometer was modified to improve temperature measurements in the flowing liquid and to optimize cooling system efficiency. Military specification hydrazine (MIL-P-26536B), filtered through a 10 micron filter was employed for the study of flow rates over a temperature profile covering 25° to 2°C. In summary, the results of the study have shown several instances of capillary orifice blockage, however, there was no evidence of gelling or thickening of the hydrazine. Blockage was believed due to particulate material. A discussion of the apparatus and results, including experimental problems, is presented in the following sections.

4.3.1 Extrusion Rheometer Test Apparatus

A schematic diagram of the extrusion rheometer utilized for this study is presented in Figure 4-6. The extrusion rheometer consists of a stainless steel cylinder of 150 cc volume, fitted with a 3/4 inch Teflon piston, a cooling jacket and the supplementary capillary section. A schematic diagram of the capillary section is presented in Figure 4-7. The capillary section consists of an 0.8 inch long glass capillary of 0.005 inch ID, a thermal conditioning chamber and cooling jacket and a thermistor (200Ω at 75°F) for temperature measurement. The thermistor output was recorded on a Sargent Model SR-5 strip chart recorder, while thermistor current was supplied utilizing a Carle Micro Detector Control. Control of the flowing liquid temperature was obtained utilizing a cold water bath circulated through both the cooling jacket of the barrel and the capillary. Hydrazine flow rate was measured by monitoring the weight of hydrazine effluent on a Torbal Torsion Balance as a function of time.

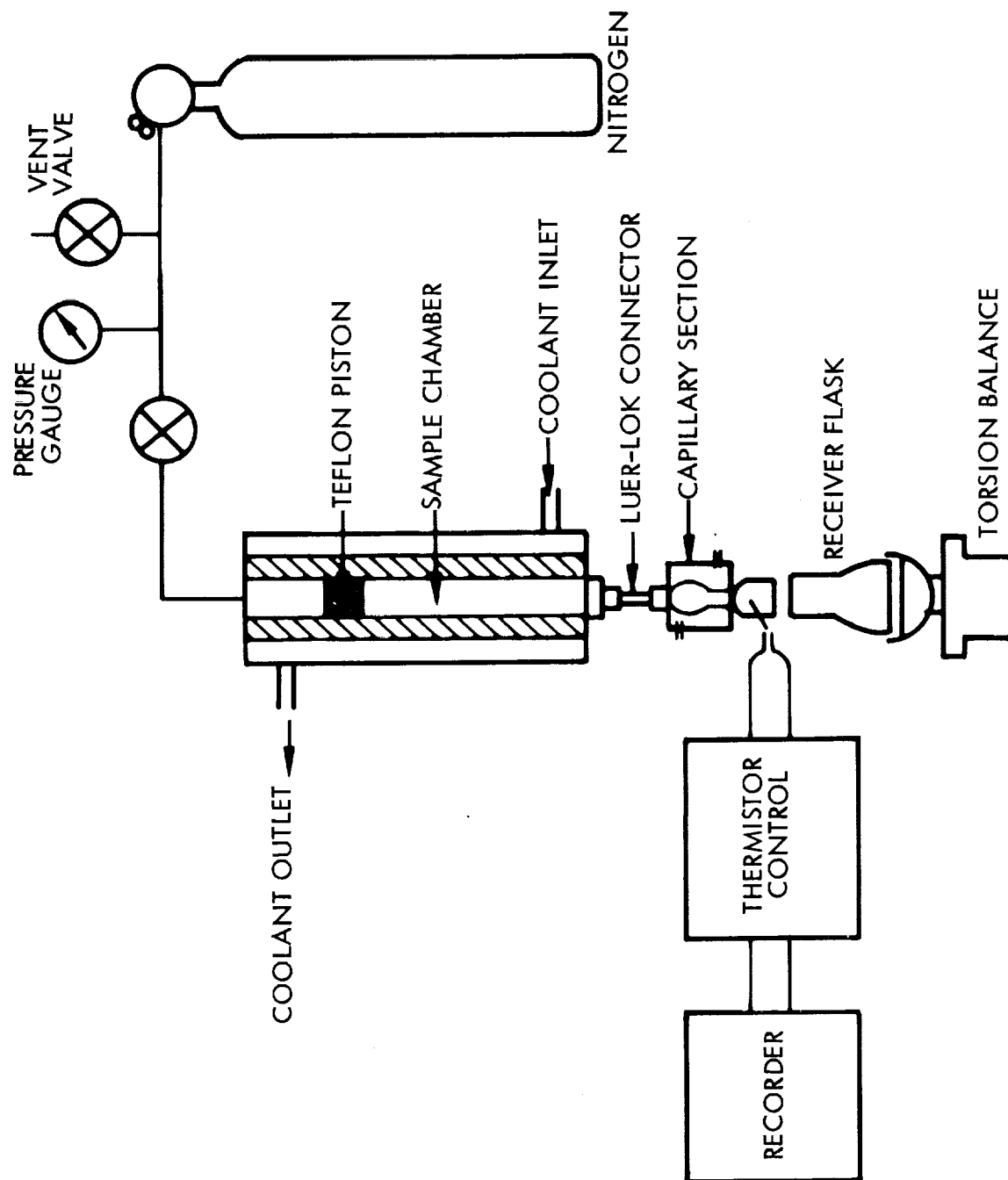


Figure 4-6. Extrusion Rheometer Setup

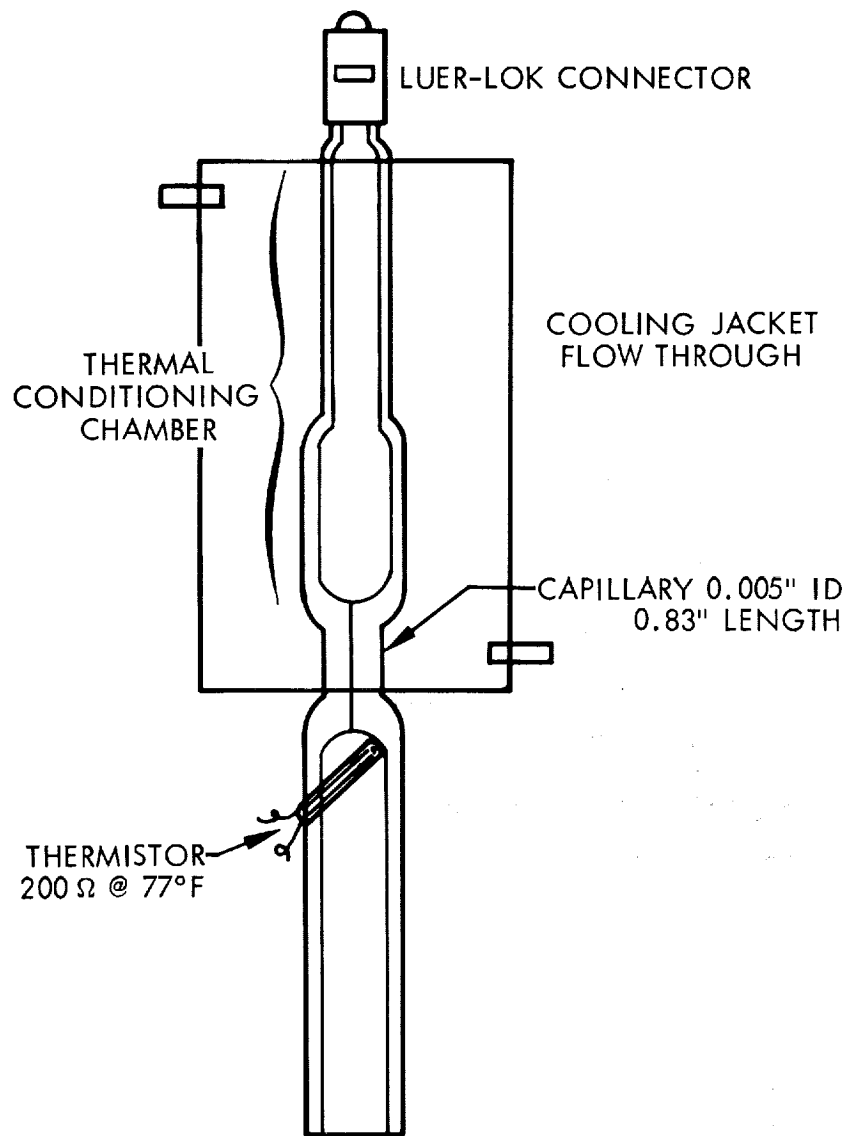


Figure 4-7. Capillary Test Section

Modifications to the previously used rheometer included substitution of the capillary section for the 0.8-inch long capillary needle (0.010-inch I.D.). The capillary section contains an auxiliary cooling jacket to increase the cooling system efficiency. The capillary section also incorporated a thermistor for measurement of flowing liquid temperature which replaced the thermocouple previously used. In addition, the flow rate measurement by weight replaced the previous volumetric measurement. The density of N_2H_4 over the temperature range of 25°C to 2°C varies less than the accuracy of the weight measurements.

Evaluation of Thermistor Temperature Measuring Concept - A test was conducted to establish the validity of using the thermistor for measuring the temperature of the flowing liquid. The apparatus was operated without fluid in the barrel but with coolant flow to observe thermistor response due to changing temperature of the walls of the capillary apparatus. The coolant was maintained at 2°C and circulated through the apparatus for 30 minutes (average run time for 100 cc hydrazine run). The thermistor recorded a slow decay in temperature from 22.6° initial to 19°C and remained constant at that point for the duration of the experiment. Confirmation of thermistor response to temperature of flowing hydrazine was obtained on subsequent hydrazine tests where the thermistor recorded temperature decay to 2°C.

4.3.2 Hydrazine Test Results

The results of a series of five runs completed with neat hydrazine are reported in Table 4-6. The volumetric flow rates reported in Table 4-6 were calculated from test data using 0.8-inch capillary length and 0.005 inch capillary diameter. Because the capillary was prepared by etching glass encased wire, the ID value is approximate. A discussion of flow rate calculations is contained in the following section.

To test the applicability of applying laminar flow equations to rheometer test results it was necessary to determine if laminar or turbulent flow existed during the experiments. Typically the criterion for the onset of turbulent flow is expressed by a dimensionless number, such as the Reynolds number. The critical Reynolds number (onset of turbulence) for

Table 4-6. Experimental Data

Run	Temperature	Tank Pressure Psig	Q (Volumetric Flow Rate) (cm ³ /sec)	% of Initial Flow Rate	Comments
1	23°C	50	0.044	100	Agrees with idealized flow data (see Table 4-7)
	10°C		0.037	84	
	2°C		0.033	75	
2	22°C	20	0.022	100	Exhibits flow decay greater than expected for fluid viscosity change
	6°C		0.014	64	
3	22°C	20	0.022	100	Exhibits flow decay greater than expected for fluid viscosity change
	16°C		0.019	86	
	12°C		0.016	73	
	8°C		0.014	64	
4	22°C	20	-	-	Initial flow erratic, capillary blockage experienced at 22°C
5	23°C	45	0.033	100	Capillary blockage experienced at 19°C
	19°C		0	0	

capillary flow of Newtonian fluids is $2100^{(2)}$. The Reynolds number calculation for run No. 1 gave a result of $R = 1,537$, indicating laminar flow. As run number one (No. 1) exhibits the highest volumetric flow rate obtained, it follows that laminar flow conditions were maintained for all experiments.

Based on this finding, an idealized set of data for change in flow rate with change in fluid viscosity was calculated utilizing laminar flow equations. The results of the calculations are presented in Table 4-7.

Table 4-7. Theoretical Hydrazine Flow Rate Data

<u>Temperature °C</u>	<u>% of 23°C Volumetric Flow Rate</u>	<u>Viscosity ² (dyne-sec/cm²)</u>
25	103	0.009049
23	100	0.009324
20	96	0.009736
15	91	0.01044
10	83	0.01118
5	78	0.01207
2	74	0.01272

The viscosity data used to calculate the idealized values were extracted from Audrieth and Ogg⁽³⁾.

By comparison of the data in Table 4-6 with the calculated flow data in Table 4-7, it is apparent that Run 1 compares well with the idealized values; Runs 2 and 3, however, show decays greater than anticipated due to increased viscosity. It is assumed that other losses due to changes in flow velocity are small as seen by comparing run No. 1 with the calculated data. Runs 4 and 5 yielded complete capillary blockage at 22° and 19°C, respectively. It should be pointed out that special precautions were taken to obviate extraneous contamination, i.e., the hydrazine used was filtered through a 10 micron millipore filter during introduction into the rheometer. Also, the capillary was cleaned by successive rinses with cleaning solution (Sat. $K_2Cr_2O_7$ in Conc. H_2SO_4), distilled H_2O and 8M NH_4OH between each flow experiment.

The rheometer capillary was dismantled at the conclusion of Run 5 and examined under a microscope. The capillary blockage was found to result from small amounts of a black solid deposited at the capillary opening and a second deposit downstream of the opening approximately 0.1 inch into the capillary tube.

In an attempt to determine the origin of the solid, distilled water rinses of all equipment used were taken for particulate counts. The counts demonstrated that the filtration procedure was reasonably efficient in removing particulate matter from the hydrazine during the loading operation. The rheometer itself, however, appeared to be a source of contamination. Although the rheometer was cleaned between runs, visual inspection of the Teflon plug and fittings after each run show signs of contamination. The black particles observed in the capillary appear to have originated in the rheometer barrel.

Calculations - The equation used to calculate relative % volumetric flow rate was

$$\% \text{ volumetric flow rate} = \frac{Q_i}{Q_{23^\circ}} \times 100$$

where: Q_1 = volumetric flow rate at temperature i

Q_{23} = volumetric flow rate at 23°C

The volumetric flow rate Q was calculated as follows:

$$Q = \frac{\pi R^4 \Delta P}{8 \eta L}$$

where: Q = volumetric flow rate in cm^3/sec

R = capillary radius in cm

P = pressure in dynes/ cm^2

L = capillary length in cm

η = viscosity in dyne-sec/ cm^2

Reynolds numbers were calculated as follows:

$$N_{Re} = \frac{2 R v_{ave} \rho}{\eta}$$

where: R = capillary radius in cm

v_{ave} = average velocity in cm/sec

ρ = fluid density in g/cm³

η = fluid viscosity in dyne-sec/cm²

REFERENCES

1. "Investigation of the Formation and Behavior of Clogging Material in Earth and Space Storable Propellants," TRW Systems Group, Interim Report 08113-6016-R000, October 1968.
2. Van Wazer, J.R., J. W. Lyons, K. Y. Kim and R. E. Colwell, "Viscosity and Flow Measurement," Interscience Publishers, New York 1963.
3. Audrieth, L. F. and B. A. Ogg, "The Chemistry of Hydrazine," John Wiley and Sons, Inc., New York, 1951.

5.0 ANALYSES OF RESULTS

This section includes a discussion and summary of the results obtained in the study of the formation of clogging materials in the liquid propellants oxygen difluoride, diborane and hydrazine. Conclusions are presented where sufficient evidence was found to verify the analysis of any anomalous flow behavior. Recommendations are given to further investigation in those areas where the results of the work performed indicated additional work.

5.1 CORROSIVITY OF OXYGEN DIFLUORIDE AND DIBORANE

5.1.1 Corrosivity of OF_2

Storage of the specimens at -78°C for 45 days in doped OF_2 has shown that the 347 stainless steel was the least attacked of the metals tested. The titanium 6Al-4V alloy showed severe damage under the test conditions using the doped propellant. The amount of corrosion deposits formed on the surfaces of the titanium specimens and capsule were believed sufficient to present a potential clogging problem. The use of 6061 aluminum alloy is uncertain, particularly in light of its behavior when stored in the 347 stainless container.

These results are applicable only under the test conditions: doped OF_2 at -78°C . It is recommended that further testing be done using neat OF_2 as well as doped OF_2 , for longer times and at various typical storage temperatures. The basis for this recommendation is as follows: (1) addition of HF to the aluminum samples indicated surface attack, (2) the possibility of interaction between dissimilar metals at -78°C indicates that there may be an upper use temperature limit that is lower than presently anticipated, and (3) a single time-temperature point does not give the type of corrosion behavior between the metals and OF_2 (linear, parabolic, logarithmic, etc.). The buildup of oxygen can be attributed to several possible reactions such as (1) reaction of OF_2 with H_2O to produce oxygen, (2) reaction of OF_2 with metal oxides, hydroxides, and hydrates found normally on metal surfaces producing hydrogen fluoride, metal fluorides and oxygen gas, and (3) the reactions (1) and (2) are not limited to storage facilities but include analyses equipment and it is not possible to determine the exact source for all O_2 .

5.1.2 Corrosivity of B_2H_6

From the results of both the corrosivity testing and the light scattering experiments, the 347 series stainless steel specimen was the least affected by neat B_2H_6 . The titanium 6Al-4V alloy was minimally attacked, while the 6061 aluminum alloy was the most affected, although to a minor degree. The most serious concern, however, are the results obtained from the B_2H_6 /stainless steel oxide experiments. The evidence of oxide surface changes, particularly with regard to the fusion of the oxide particles and possible reduction of the oxide to metal, indicates a potential problem area with respect to propellant components where galling and/or cold welding may occur. It is recommended that further testing of metal oxides with diborane be performed. These tests should include both static compatibility tests as well as dynamic testing under simulated operating conditions.

5.2 CHARACTERIZATION OF OXYGEN DIFLUORIDE AND DIBORANE

5.2.1 Characterization of OF_2

The purpose of characterization of the propellant after storage in the presence of metal storage containers and test coupons, see Section 2.4, was to determine if these metals and dopants produced impurities in the liquid which might contribute to flow decay. The laser examination and analyses of the vapor showed no new materials which might be construed to cause flow decay. However, the method of laser analysis was not ideal. It was not considered safe to transfer the liquid by direct bleeding to the laser viewing tube for examination; non-volatile suspendable material was not transferred by vacuum manipulation to the laser viewing tube. Any residues, however, remained in the storage conditioning tube and were recoverable. Except for tightly adhering residues on titanium, no residues were obtained.

Analysis of the propellant, as described in Section 3.2.1, which was recovered from the stored samples showed no change in impurities except for oxygen content. The residual water and hydrogen fluoride was purposely left out of the analyses. They were transferred into the conditioning tubes in a method that prevented these dopants from contacting the propellant

above -78°C . The propellant was also removed while the tubes were chilled at -78°C to prevent higher temperature reactions not applicable to these storage conditions. In this way, it was possible to determine if the water and hydrogen fluoride were consumed at -78°C . In all cases the water was consumed and not recoverable. The hydrogen fluoride was consumed completely in the conditioning tube constructed of aluminum 6061-T6 and the aluminum sample. Hydrogen fluoride was partially recoverable from all other samples, even from the 6061-T6 aluminum specimen stored in the 347 stainless steel bomb. As pointed out in Section 3.2.1, difficulty was encountered when the aluminum 6061-T6 conditioning tube with a similar metal coupon was being loaded with hydrogen fluoride at -78°C . The frozen water vapor was already present in the tube at this stage and the hydrogen fluoride reacted rapidly to form a non-condensable gas, probably hydrogen. It was necessary to evacuate the system and attempt to add hydrogen fluoride several times before the system could be doped at the same level of condensed gas as with the other samples. The fact that hydrogen fluoride was recoverable in part from the 6061-T6 aluminum sample in the stainless steel bomb may be related to total surface.

Because the water was consumed it is reasonable to assume that part of the oxygen increase is attributable to the replacement of hydrogen in water with fluoride to produce hydrogen fluoride and O_2 gas. As a result of doping all samples at the same concentration level, it could be assumed that oxygen from water would be released in equal amounts from this source, yet the oxygen analyses are not the same in all samples. It must be concluded that some oxygen comes from other sources. This would be from replacement of oxygen in surface metal oxides and preferential reaction of fluorine from OF_2 with metals and oxides to produce oxygen from the OF_2 . These reactions are favored thermodynamically. The buildup of oxygen is of particular importance to the storage of OF_2 in space because oxygen, even though very soluble in OF_2 and unlikely to cause flow decay, could increase the pressure in the storage vessel. The oxygen critical pressure is below -140°C .

There is little evidence that fluorine or oxygen difluoride reaction with metals ever ceases, the reaction with most metals slows down with a buildup of a non-volatile protective coating. This coating is protective only if

it is soluble in the liquid and adheres firmly to the underlying metal. The absence of solid crystals, with the exception of titanium in the conditioning tubes, indicates a limited solubility of the fluorides of metals studied in OF_2 at -78°F . This storage period of 45 days is not sufficiently long to determine the usefulness of these metals for long term storage.

Because the normal impurities such as CO_2 , SiF_4 , and HF are solids below -78°C , the tolerable limit for these materials must be established in determining specification for OF_2 .

5.2.2 Characterization of B_2H_6

The mass spectrometric analysis identified hydrocarbons and isopropoxy-pentaborane as impurities in the diborane sample used for this study. The other minor impurities, N_2 , O_2 and CO_2 are air impurities introduced during synthesis or transfer. As pointed out, the source of the pentaborane impurity is unknown and not often found in diborane. Hydrocarbons are normal impurities in diborane and come from reduction of ethers or solvents used in preparing the fuel. That these impurities can produce precipitates in the liquid range is very important to flow control. The demonstration that a Tyndall effect was present throughout the liquid range studied points out that these impurities should be eliminated. The observed increase in Tyndall effect with decreasing temperature suggests that these impurities must be considered in preparing specification for diborane impurity.

If diborane contained impurities formed by the storage in the conditioning tubes which were not reasonably volatile, mass spectrometric analyses would not have detected them. Examples of materials likely to be undetected would be partially hydrolyzed diborane, boric acid or boric oxide. Their solubility in liquid diborane is unknown and undetermined by these studies. The change in surface characteristics of the stored metal samples and especially the results of the stainless steel oxides suggests that oxides can be reduced. Thus an equivalent amount of diborane oxidation products would be produced.

At the storage temperature of -78°C , very little pyrolysis took place as evidenced by the absence of higher hydrides. The hydrogen produced can be from the reaction of diborane with metal oxides, hydroxides or hydrolysis of traces of water.

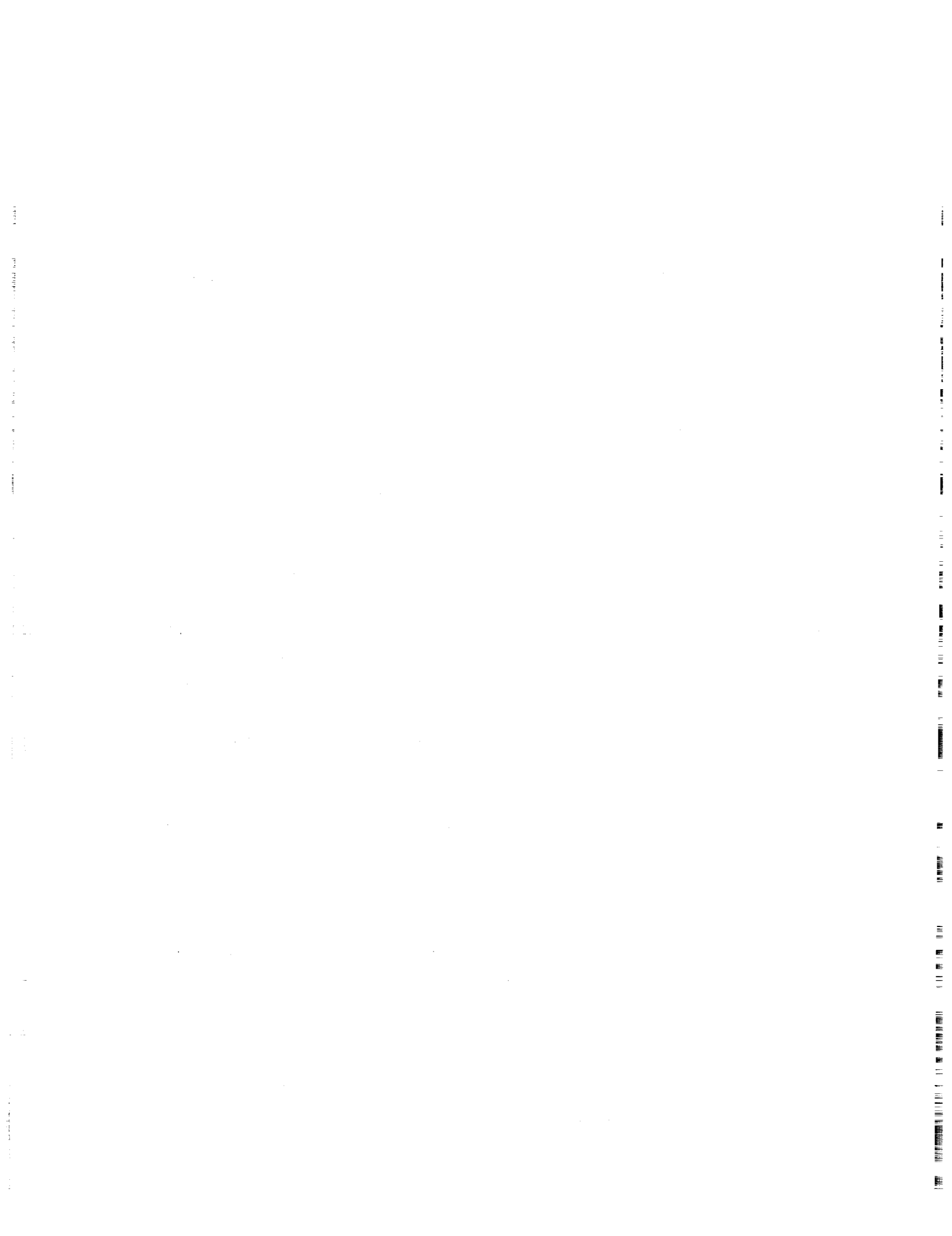
The presence of pyrolysis solids, the classical yellow solids which analyze as $(\text{BH})_x$, was not encountered here but could be a very difficult problem if diborane passed through heated valves or contacted against hot surfaces.

5.3 PROPELLANT FLOW TESTING

5.3.1 Oxygen Difluoride Flow Tests

The lack of demonstrated flow decay under the conditions studied with neat and concentrated or doped propellant is by no means conclusive. While effort was made to examine small quantities (2 cc) of propellants stored for 45 days for corrosion products which might cause flow decay, the propellant actually tested was neat. The storage and transfer of sufficient conditioned propellant as a liquid to the flow apparatus would have required much more equipment and effort and would have been considerably more dangerous to handle. This tested propellant was in the apparatus only a few hours during the flow tests. Passivation of the entire apparatus at room temperature with fluorine-oxygen mixture prior to flow testing most likely produced a thicker fluoride coating on the walls than could be expected at -140°C with the neat propellant during this short exposure. The room temperature passivation of the flow system was a safety measure to burn off any oxidizable residues and may produce an entirely different surface than neat OF_2 at -140°C .

Perhaps a more serious problem is the effect of long term storage (2, 5, 10 and 15 years) on possible production of crystalline residues in the liquid. Long term storage could produce conditions favoring extractive leaching or even extremely insoluble fluoride residues. Resultant crystals could grow in size. High velocity flow may accelerate this extractive process. There is no evidence that corrosion with fluorine oxidizers ever terminates. The reaction slows due to the formation of protecting metal fluoride surfaces. If these surfaces are even partially soluble in the liquid, problems can develop.



5.3.2 Diborane Flow Tests

The lack of evidence of flow decay of liquid B_2H_6 in stainless steel apparatus is not surprising since stainless appeared to very inert to B_2H_6 in storage. The observation that stainless steel oxides can be reduced or altered by storage in B_2H_6 , however, suggests that the metal containers should contain freshly polished surfaces. There have been reports of boron hydrides causing surface cracks in maraging steels* but no reported difficulties with stainless steel equipment. The potential to reduce metals is apparent and it will be important to determine if the reduced metal can dislodge from surfaces.

The demonstrated reaction of diborane with stainless steel oxides was an "accelerated test" because the sample was stored at $-20^{\circ}C$, well above the proposed propellant storage temperature, but this suggests that reduction can take place on stainless steel surfaces which always contain oxides. This reduction should involve only a few molecular layers, yet the resultant oxides of boron might interfere with flow. Preliminary reduction of these surfaces, similar to fluorine passivation, may be indicated. It may not be necessary to use boron hydrides for passivation. Reducing agents which do not produce solid residues, such as hydrogen gas at elevated temperatures, may be more effective as a passivation method.

Complete elimination of water from storage equipment is mandatory because of hydrolysis of diborane to boron oxides and boric acid. Halogenated solvents and cleaning agents containing labile chlorine atoms should be avoided for cleaning at elevated temperatures because of the possible formation of metal chlorides. Partially hydrolyzed aluminum chloride, for example, was found to act as a gelling agent for boron hydrides.

These observations were made under the High Energy Liquid Boron Hydrides Program (ZIP) in attempting to destroy aluminum chloride catalysts in Friedel-Crafts alkylation experiments with boron hydrides. Ferric chloride is a similar catalytic material which can react with water to form hydrated colloidal particles. The reaction of diborane with this class of materials

* Private Communication with Dr. Tiner, MacDonnell Douglas Corporation.

would be a suspected source of possible flow decay. These chlorides are very soluble in the higher hydrides such as decaborane and pentaborane. Limited solubility of ferric chloride in liquid diborane would also be expected.

In this study, the diborane was shown by laser examination to contain suspended material and concentration increased with decreasing temperature. This suggests that soluble materials were being precipitated during the cooling cycle. Expansion cooling at an orifice or capillary exhaust could cause similar precipitation. To help eliminate suspended material from entering the capillary test section, the filter element (5 micron holes) was placed directly in front of the capillary test section.

Methods such as doping and temperature cycling can aid in determining if a problem exists. By maintaining the temperature of the propellant in the hold tank and cooling at the entrance of the capillary, precipitation of any clogging material can be found.

5.3.3 Hydrazine Flow Tests

The tests performed demonstrated that the flow rate decay expected on the basis of viscosity change with temperature, can be measured accurately if spurious contamination of the capillary is prevented. In those instances where flow degradation exceeded the expected values with relatively pure specification grade hydrazine and complete blockage was not experienced, (Runs 2 and 3), no apparent cause was identified. Under no circumstances was the fuel observed to gel or thicken.

Although special precautions were taken to eliminate extraneous contamination, it would appear that exposure of the internal walls of the rheometer barrel to hydrazine resulted in dislodging of particles which were not removed by flushing with water. It is possible that all observed flow clogging behavior can be attributed to deposition of dislodged particles at the capillary entrance. In selecting the 5 mil capillary size, it was hoped to exaggerate any flow clogging phenomena. The relative ease with which this capillary was plugged with neat hydrazine suggests that future flow experiments with doped hydrazine should be conducted with larger capillaries.

